

# Haptic Sensors & Interfaces for Robotic Telemanipulation

Emil M. Petriu, Dr. Eng., FIEEE  
Ana-Maria Cretu, M.A.Sc., Ph.D. candidate  
School of Information Technology and Engineering  
University of Ottawa  
Ottawa, ON., K1N 6N5 Canada  
<http://www.site.uottawa.ca/~petriu>

## Abstract

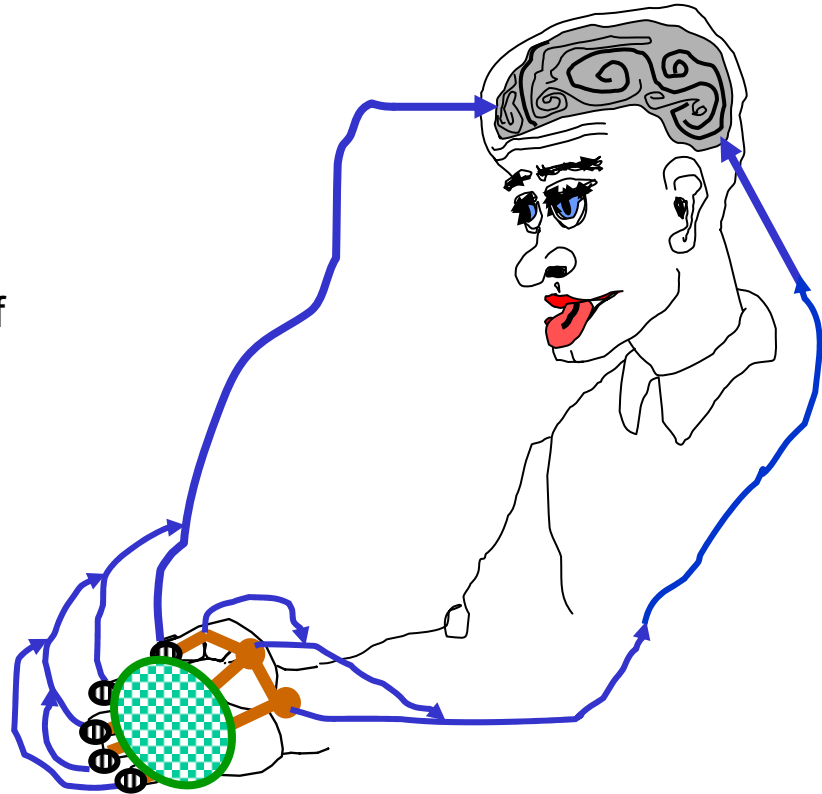
The tutorial will discuss development issues of the *human-computer* and *computer-robot* haptic interfaces for robotic telemanipulation:

- human haptic perception;
- robot haptic perception;
- haptic interfaces for object manipulation in interactive virtual environments and robotic telemanipulation systems;
- composite geometric & haptic object models which are conformal representations of real objects, accounting for their geometric shape and elastic behaviour while interacting through direct contact with other objects;
- experimental results.

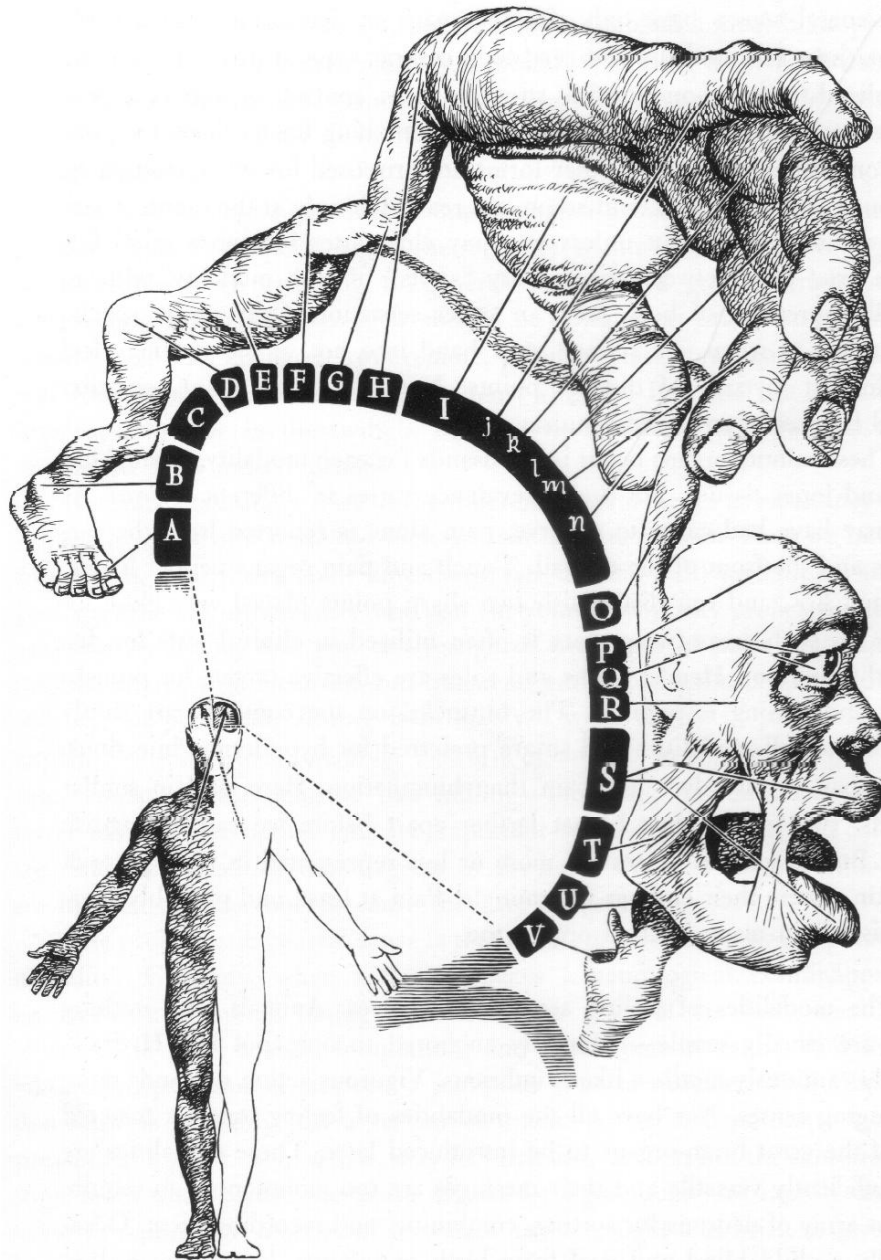
## ***Human Haptic Perception***

Human haptic perception is the result of a complex dexterous manipulation act involving two distinct components:

- (i) **cutaneous** information from touch sensors which provide about the geometric shape, contact force, elasticity, texture, and temperature of the touched object area. The highest density of cutaneous sensors is found in **fingerpads** (but also in the **tongue**, the **lips**, and the foot). Force information is mostly provided by sensors on **muscles**, **tendons** and **bone joints** proprioceptors;
- (ii) **kinesthetic** information about the positions and velocities of the **kinematic structure** (**bones and muscles**) of the hand



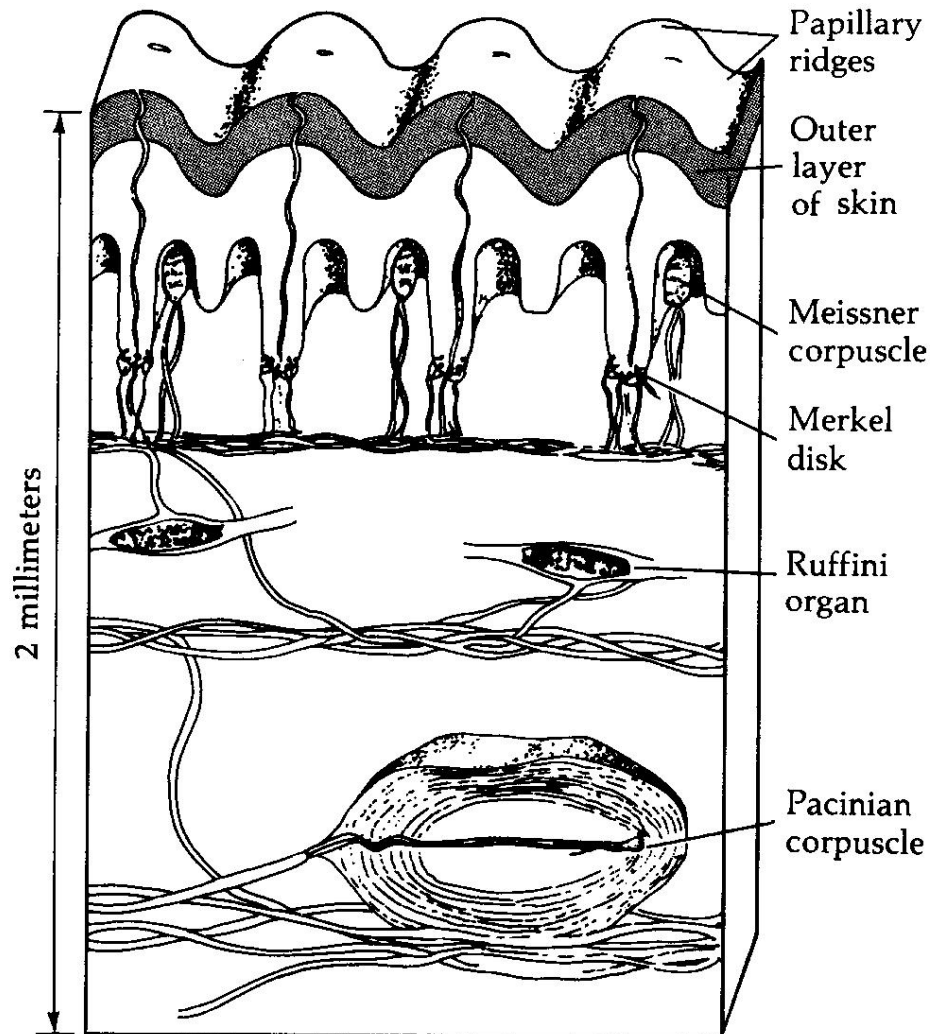
“In a way, touch can be constructed as the most reliable of the [human] sensor modalities. When the senses conflict, touch is usually the ultimate arbiter. ... Touch sensations can arise from stimulation anywhere on the body’s surface. Indeed, the **skin can be characterized as one large receptor surface for the sense of touch.** ... The English neurologist H. Jackson paid homage to the wonderful and complex abilities of the *human hand* by calling it *the most intelligent part of the body*. The skin on the human hand contains thousands of **mechanoreceptors** (sensitive to mechanical pressure of deformation of the skin), as well as a **complex set of muscle to guide the fingers** as they explore the surface of an object. The mechanoreceptors play a key role in analyzing object detail such as texture; the muscles make their big contribution when grosser features such as size, weight, and shape are being analyzed. But, whether exploring gross or small details, the **hand and the finger pads convey the most useful tactile information about objects.** In this respect, the hand is analogous to the eye’s fovea, the region of retina associated with keen visual acuity. There is, however, a flaw in this analogy: fovea vision is most acute when the eye is relatively stationary, but **touch acuity is best when the fingers move of the object of regard**” (from [R. Sekuler, R. Balke, *Perception*, 2nd edition, McGraw-Hill, NY, 1990, Chapter 11. Touch, pp. 357-383]).



**The sensory cortex:** an oblique strip, on the side of each hemisphere, receives sensations from parts on the opposite side of the body and head: foot (A), leg (B, C), hip (D), trunk (E), shoulder (F), arm (G, H), hand (I, J, K, L, M, N), neck (O), cranium (P), eye (Q), temple (R), lips (S), cheek (T), tongue (U), and larynx (V). Highly sensitive parts of the body, such as the hand, lips, and tongue have proportionally large mapping areas, the foot, leg, hip, shoulder, arm, eye, cheek, and larynx have intermediate sized mapping areas, while the trunk, neck, cranium, and temple have smaller mapping areas.

(from [H. Chandler Elliott, *The Shape of Intelligence - The Evolution of the Human Brain*, Drawings by A. Ravielli, Charles Scribner's Sons, NY, 1969])

## Cutaneous Sensing



### Cutaneous sensors:

The highest density of cutaneous sensors is found in fingertips, but also in the foot soles, the tongue, and the lips.

**Force information** is mostly provided by sensors on muscle tendons and bones/joints proprioceptors;

◁ **Cross section through the skin of primate finger pad** showing the location of specialized nerve fiber terminals (from [R. Sekuler, R. Balke, *Perception*, 2<sup>nd</sup> edition, McGraw-Hill, NY, 1990]).

[Burdea & Coiffet 2003] G. Burdea and Ph. Coiffet, Virtual Reality Technology, (2<sup>nd</sup> edition), Wiley, New Jersey, 2003

**Cutaneous sensors =>**

- 40 % are *Meissner's corpuscles* sensing velocity and providing information about the movement across the skin;
- 25% are *Merkel's disks* which measure pressure and vibrations;
- 13 % are *Pacinian corpuscles* (buried deeper in the skin) sensing acceleration and vibrations of about 250 Hz;
- 19% are *Rufini corpuscles* sensing skin shear and temperature changes.

*[Burdea & Coiffet 2003]* Comparison of various skin mechanoreceptors

<b>Receptor Type</b>	<b>Rate of Adaptation</b>	<b>Stimulus frequency (Hz)</b>	<b>Receptive Field</b>	<b>Function</b>
Merkel Disks	SA-I	0–10	Small, well defined	Edges, intensity
Ruffini Corpuscles	SA-II	0–10	Large, indistinct	Static force, skin stretch
Meissner Corpuscles	FA-I	20–50	Small, well defined	Velocity, edges
Pacinian Corpuscles	FA-II	100–300	Large, indistinct	Acceleration, vibration

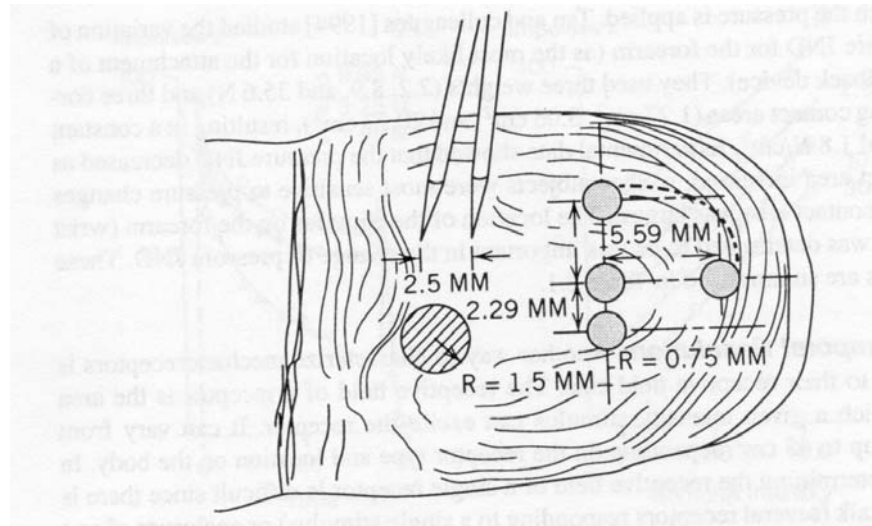
Based on Seow [1988], Cholewiak and Collins [1991], and Kalawsky [1993]



## Spatial resolution

[Burdea & Coiffet 2003]

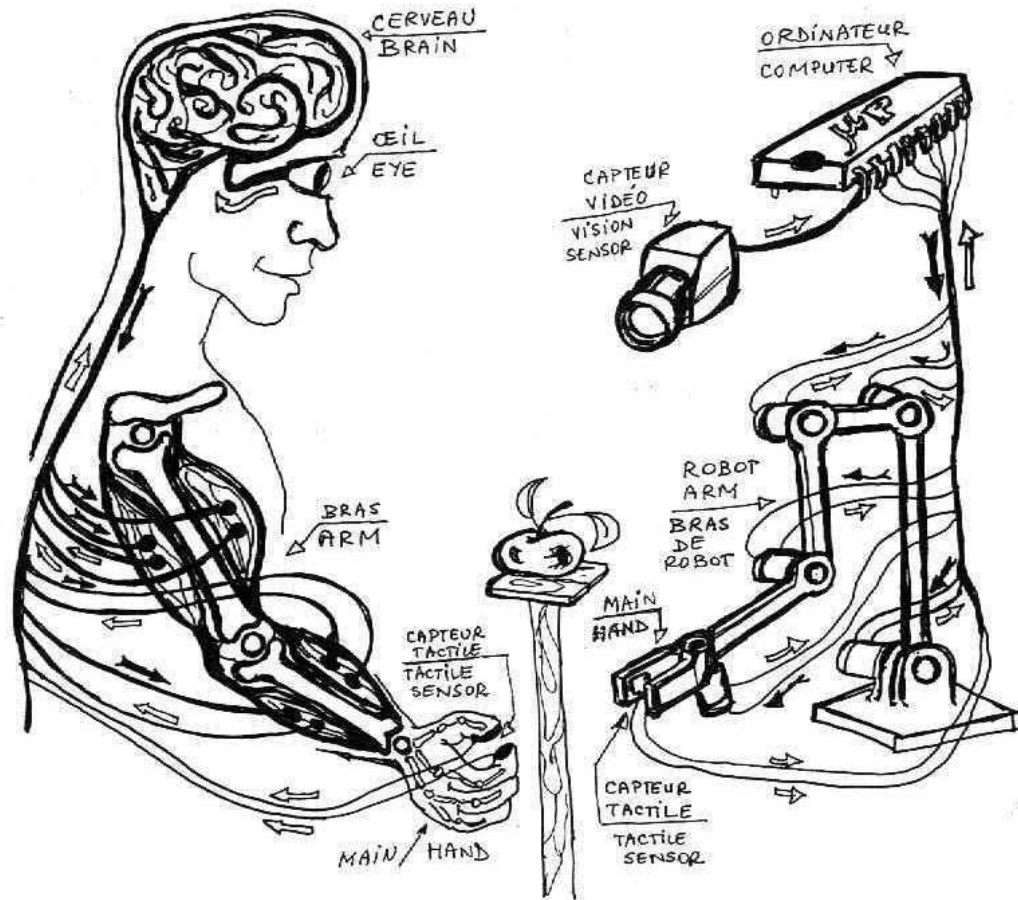
- If the sensor has a large receptive field – it has low spatial resolution (Pacinian and Ruffini)
- If the receptive field small - it has high spatial resolution (Meissner and Merkel)



Two-point limen test: 2.5 mm fingertip, 11 mm for palm, 67 mm for thigh (from [Burdea & Coiffet 2003]).

## Robot Haptic Sensors

Robot haptic sensing mechanisms emulate those of the humans.

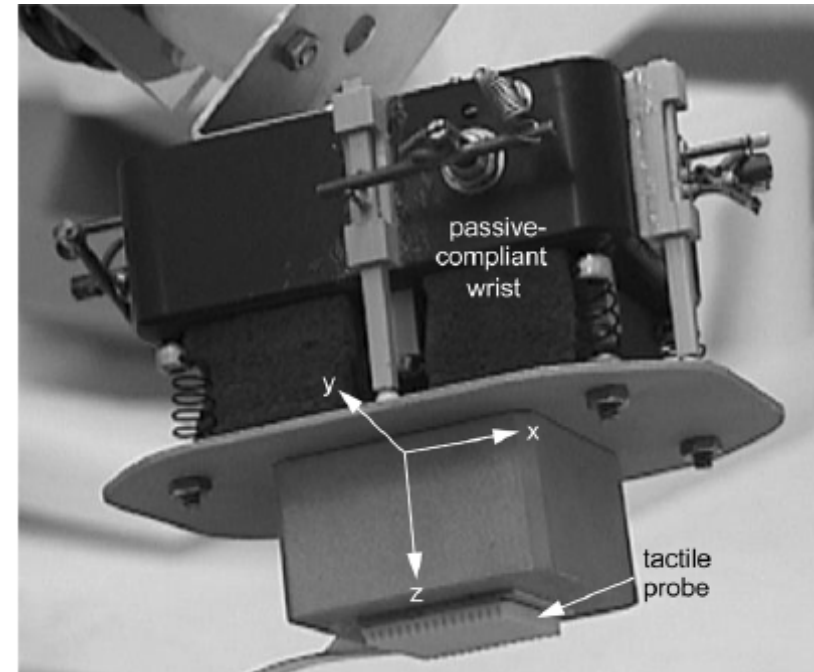


**Haptic perception is the result of an active deliberate contact exploratory sensing act.**

A **tactile probe** provides the local “cutaneous” information about the touched area of the object.

A **robotic carrier** providing the “kinesthetic” capability is used to move the tactile probe around on the explored object surface and to provide the contact force needed for the probe to extract the desired cutaneous information (e.g. local 3D geometric shape, elastic properties, and/or termic impedance) of the touched object area .

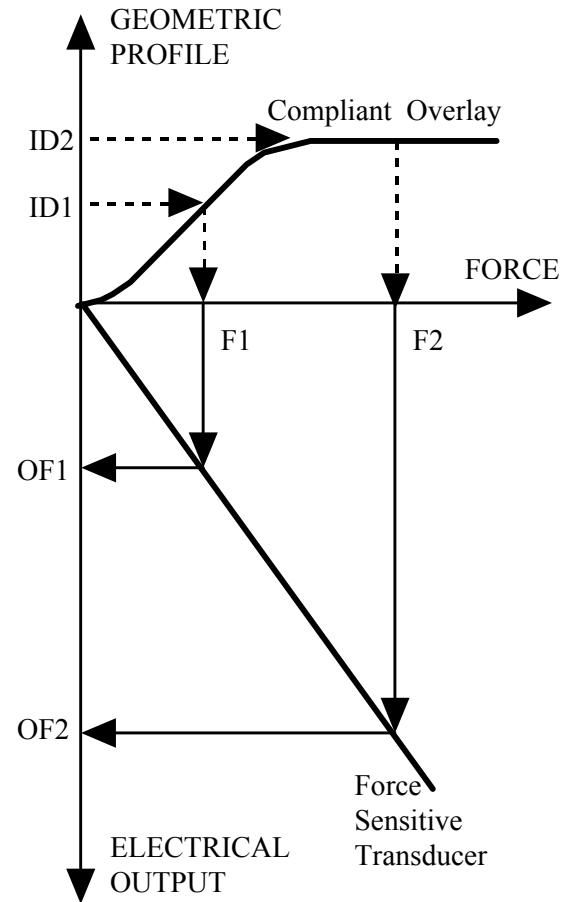
The local *information provided by the tactile probe is integrated with the kinesthetic position parameters of the carrier* resulting in a composite **haptic model** (global geometric and elastic profiles, termic impedance map) of the explored 3D object.

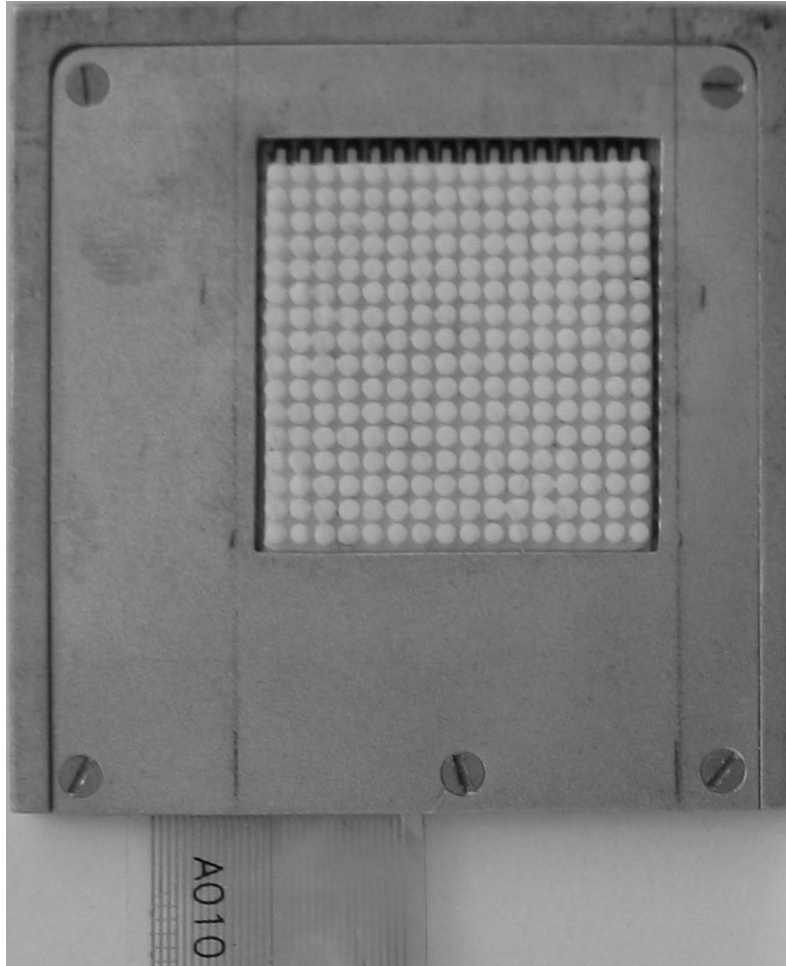


**Biology-inspired robot haptic perception system** consists of a robot “finger”, an instrumented **passive-compliant wrist** and a **tactile probe** array. Position sensors placed in the robot joints and on the instrumented passive-compliant wrist provide the kinesthetic information. The compliant wrist allows the probe to accommodate the constraints of the touched object surface and thus to increase the local cutaneous information extracted during the active exploration process under the force provided by the robot.  
(from [E.M. Petriu, W.S. McMath, S.K. Yeung, N. Trif, "Active Tactile Perception of Object Surface Geometric Profiles," *IEEE Trans. Instrum. Meas.*, Vol. 41, No. 1, pp.87-92, 1992. ]).

## Tactile probe for rigid object inspection.

It consists of a force sensitive transducer and an elastic overlay that provides a *geometric profile-to-force* transduction function .





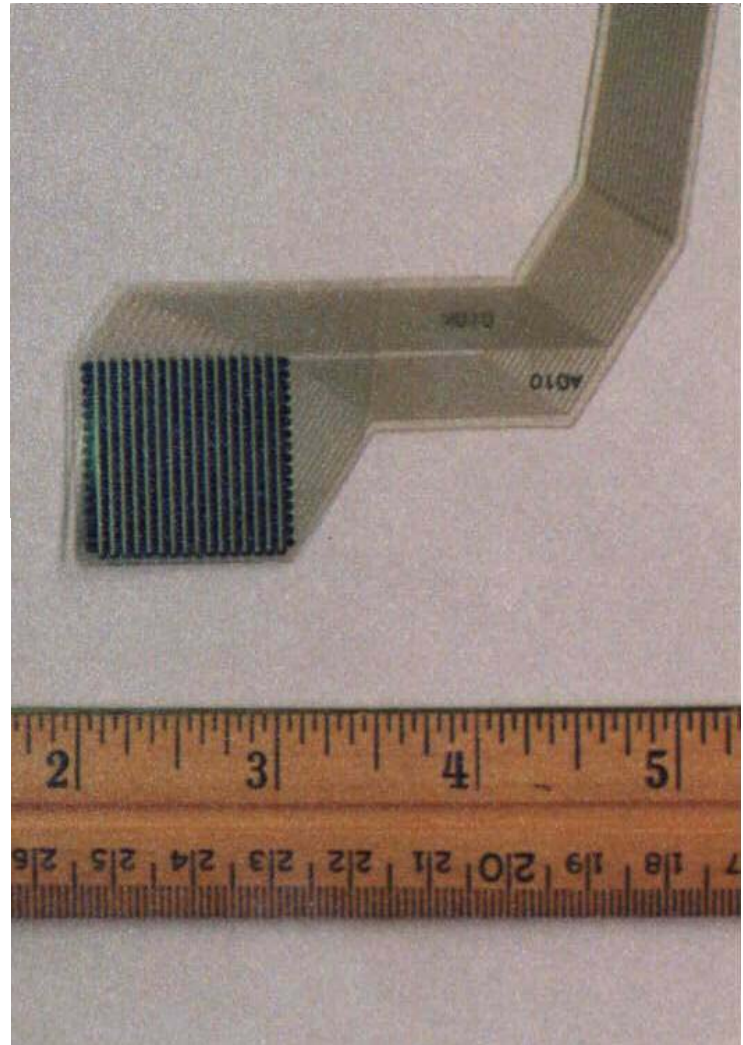
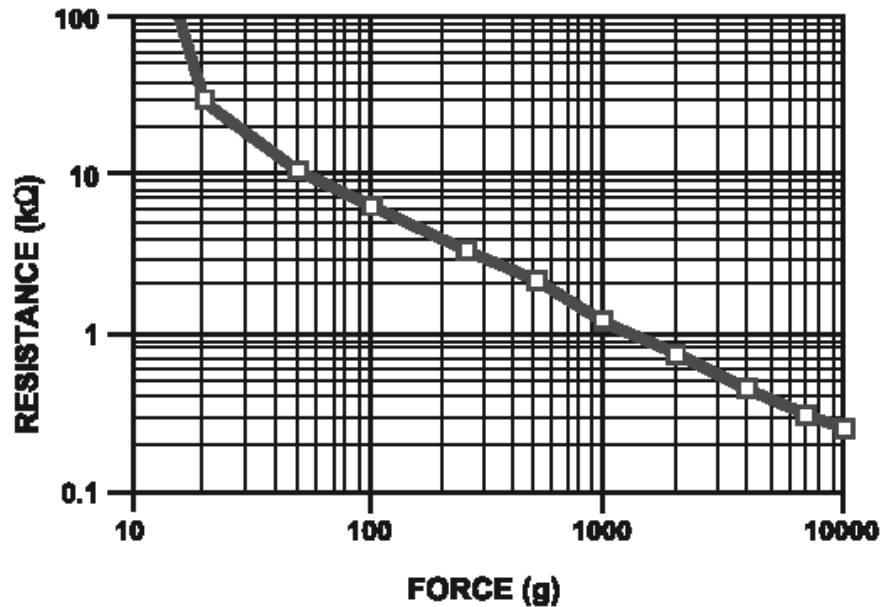
**Tactile Probe** developed for the *Canadian Space Agency* in the early 90s.

The tabs of the elastic overlay are arranged in a 16-by-16 array having a tab on top of each node of the *FSR* matrix.

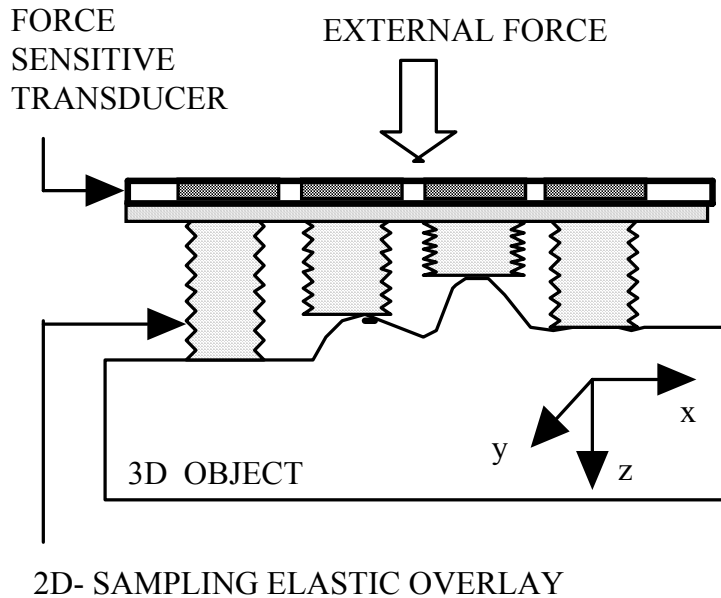
This tab configuration provides a *de facto* spatial sampling, which reduces the elastic overlay's blurring effect on the high 2D sampling resolution of the *FSR* transducer. (from [ S.K. Yeung, E.M. Petriu, W.S. McMath, D.C. Petriu, "High Sampling Resolution Tactile Sensor for Object Recognition," *IEEE Trans. Instrum. Meas.*, Vol. 43, No. 2, pp.277-282, 1994] )

The tactile probe is based on a 16-by-16 matrix of **Force Sensing Resistor (FSR)** elements spaced 1.58 mm apart on a 6.5 cm<sup>2</sup> (1 sq. inch) area.

The FSR elements have an exponentially decreasing electrical resistance with applied normal force: the resistance changes by two orders of magnitude over a pressure range of 1 N/cm<sup>2</sup> to 100 N/cm<sup>2</sup>.



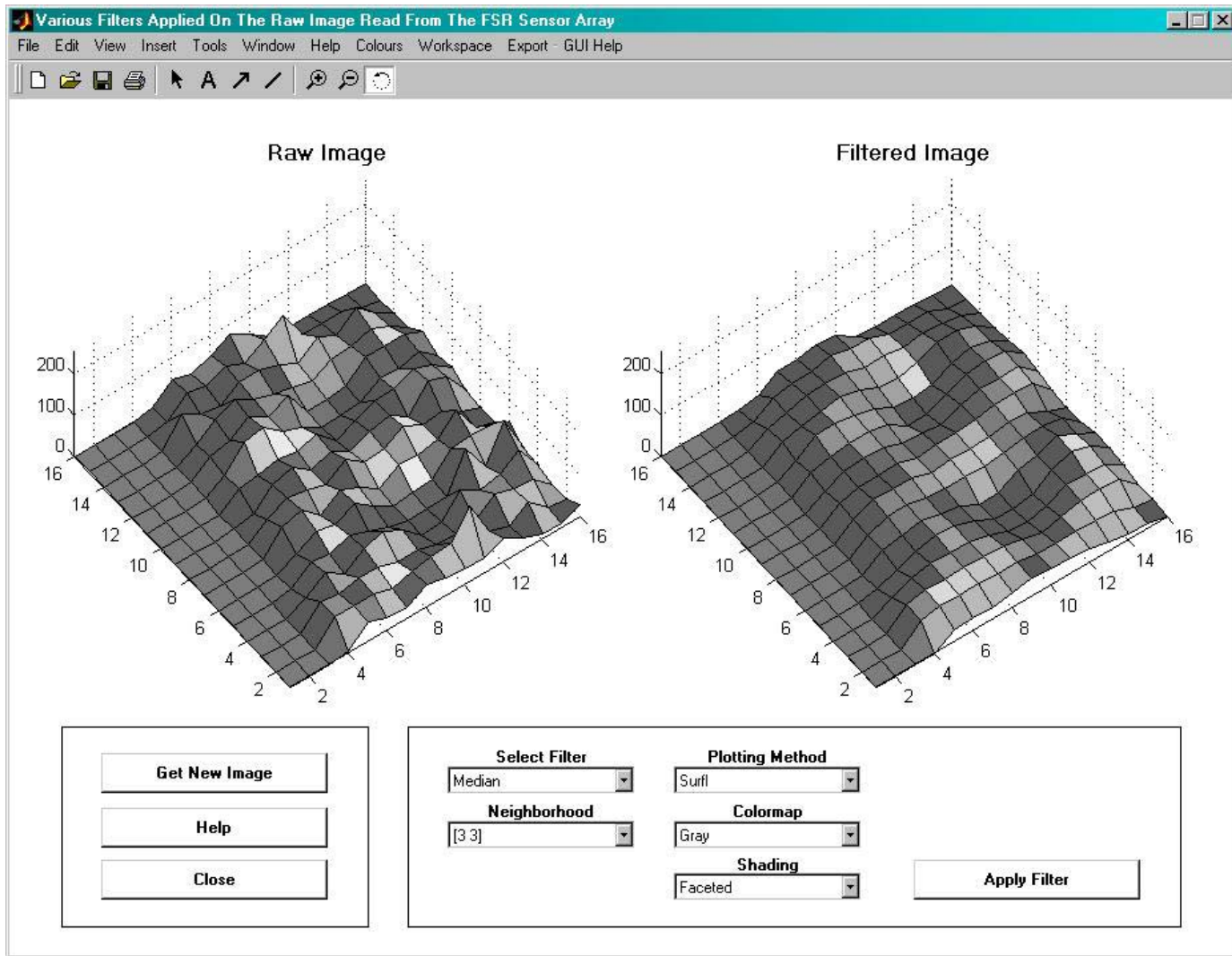




The **elastic overlay** has a protective damping effect against impulsive contact forces and its elasticity resets the transducer when the probe ceases to touch the object.

The crosstalk effect present in one piece elastic pads produces considerable blurring distortions. It is possible to reduce this by using a *custom-designed elastic overlay* consisting of a relatively thin membrane with protruding round tabs. This construction allows free space for the material to expand in the x and y directions allowing for a compression in the z direction proportional with the stress component along this axis.





Example of GUI window (from [C. Pasca, *Smart Tactile Sensor*, M.A.Sc. Thesis, University of Ottawa, 2004])

# Robotic Model-Based Tactile Recognition of Pseudo-Random Encoded 3D Objects

[ E.M. Petriu, S.K.S. Yeung, S.R. Das, A.M. Cretu, H.J.W. Spoelder, "Robotic Tactile Recognition of Pseudorandom Encoded Objects, IEEE Trans. Instrum. Meas., Vol.53, No.5, pp.1425-1432, 2004.]

Pseudo-Random Binary Encoding provide a practical solution allowing absolute position recovery with any desired  $n$ -bit resolution while employing only one binary track, regardless of the value of  $n$ .

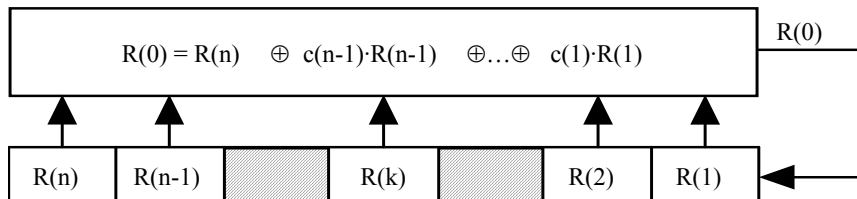


Table 1 Feedback equations for PRBS generation

Shift register length $n$	Feedback for direct PRBS	Feedback for reverse PRBS
	$R(0) = R(n) \oplus c(n-1) \cdot R(n-1) \oplus \dots \oplus c(1) \cdot R(1)$	$R(n+1) = R(1) \oplus b(2) \cdot R(2) \oplus \dots \oplus b(n) \cdot R(n)$
4	$R(0) = R(4) \oplus R(1)$	$R(5) = R(1) \oplus R(2)$
5	$R(0) = R(5) \oplus R(2)$	$R(6) = R(1) \oplus R(3)$
6	$R(0) = R(6) \oplus R(1)$	$R(7) = R(1) \oplus R(2)$
7	$R(0) = R(7) \oplus R(3)$	$R(8) = R(1) \oplus R(4)$
8	$R(0) = R(8) \oplus R(4) \oplus R(3) \oplus R(2)$	$R(9) = R(1) \oplus R(3) \oplus R(4) \oplus R(5)$
9	$R(0) = R(9) \oplus R(4)$	$R(10) = R(1) \oplus R(5)$
10	$R(0) = R(10) \oplus R(3)$	$R(11) = R(1) \oplus R(4)$

$n$	$q=3$	$q=4$	$q=8$	$q=9$
2	$x^2+x+2$	$x^2+x+A$	$x^2+Ax+A$	$x^2+x+A$
3	$x^3+2x+1$	$x^3+x^2+x+A$	$x^3+x+A$	$x^3+x+A$
4	$x^4+x+2$	$x^4+x^2+Ax+A^2$	$x^4+x+A^3$	$x^4+x+A^5$
5	$x^5+2x+1$	$x^5+x+A$	$x^5+x^2+x+A^3$	$x^5+x^2+A$
6	$x^6+x+2$	$x^6+x^2+x+A$	$x^6+x+A$	$x^6+x^2+Ax+A$
7	$x^7+x^6+x^4+1$	$x^7+x^2+Ax+A^2$	$x^7+x^2+Ax+A^3$	$x^7+x+A$
8	$x^8+x^5+2$	$x^8+x^3+x+A$		
9	$x^9+x^7+x^5+1$	$x^9+x^2+x+A$		
10	$x^{10}+x^9+x^7+2$	$x^{10}+x^3+A(x^2+x+1)$		

The following relations apply:

for  $GF(4) = GF(2^2)$ :

$$A^2+A+1=0, A^2=A+1, \text{ and } A^3=1$$

for  $GF(8) = GF(2^3)$ :

$$A^3+A+1=0, A^3=A+1, A^4=A^2+A, A^5=A^2+A+1, \\ A^6=A^2+1, \text{ and } A^7=1$$

for  $GF(9) = GF(3^2)$ :

$$A^2+2A+2=0, A^2=A+1, A^3=2A+1, A^4=2, A^5=2A, \\ A^6=2A+2, A^7=A+2, \text{ and } A^8=1$$

According to the PRMVS window property any q-valued contents observed through a n-position window sliding over the PRMVS is unique and fully identifies the current position of the window.

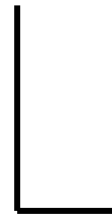
0	A	1	A <sup>2</sup>	A	A <sup>2</sup>	A <sup>2</sup>	A <sup>2</sup>	1	1	A <sup>2</sup>	A <sup>2</sup>	A <sup>2</sup>	A	A <sup>2</sup>	1	A
0	0	1	A <sup>2</sup>	A <sup>2</sup>	A	1	0	A <sup>2</sup>	A <sup>2</sup>	0	1	A	A <sup>2</sup>	A <sup>2</sup>	1	0
0	A <sup>2</sup>	0	0	A	A	A <sup>2</sup>	1	A <sup>2</sup>	A <sup>2</sup>	1	A <sup>2</sup>	A	A	0	0	A <sup>2</sup>
0	1	A	1	A	0	A <sup>2</sup>	A	0	0	A	A <sup>2</sup>	0	A	1	A	1
0	A <sup>2</sup>	A <sup>2</sup>	A	0	A <sup>2</sup>	0	1	1	1	1	0	A <sup>2</sup>	0	A	A <sup>2</sup>	A <sup>2</sup>
0	A <sup>2</sup>	A	1	A <sup>2</sup>	1	1	1	A	A	1	1	1	A <sup>2</sup>	1	A	A <sup>2</sup>
0	0	A	1	1	A <sup>2</sup>	A	0	1	1	0	A	A <sup>2</sup>	1	1	A	0
0	1	0	0	A <sup>2</sup>	A <sup>2</sup>	1	A	1	1	A	1	A <sup>2</sup>	A <sup>2</sup>	0	0	1
0	A	A <sup>2</sup>	A	A <sup>2</sup>	0	1	A <sup>2</sup>	0	0	A <sup>2</sup>	1	0	A <sup>2</sup>	A	A <sup>2</sup>	A
0	1	1	A <sup>2</sup>	0	1	0	A	A	A	A	0	1	0	A <sup>2</sup>	1	1
0	1	A <sup>2</sup>	A	1	A	A	A	A <sup>2</sup>	A <sup>2</sup>	A	A	A	1	A	A <sup>2</sup>	1
0	0	A <sup>2</sup>	A	A	1	A <sup>2</sup>	0	A	A	0	A <sup>2</sup>	1	A	A	A <sup>2</sup>	0
0	A	0	0	1	1	A	A <sup>2</sup>	A	A	A <sup>2</sup>	A	1	1	0	0	A
0	A <sup>2</sup>	1	A <sup>2</sup>	1	0	A	1	0	0	1	A	0	1	A <sup>2</sup>	1	A <sup>2</sup>
0	A	A	1	0	A	0	A <sup>2</sup>	A <sup>2</sup>	A <sup>2</sup>	A <sup>2</sup>	0	A	0	1	A	A

15-by-17 PRA obtained by folding a 255 element PRS defined over GF(4), with  $q=4$ ,  $n=4$ ,  $k_1=2$ ,  $k_2=2$ ,  $n_1=q^{k_1}-1=15$ , and  $n_2=(q^n-1)/n_1=17$

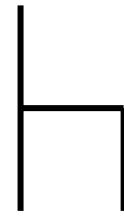
The shape of the embossed symbols is specially designed for easy tactile recognition. For an efficient pattern recognition, the particular shape of the binary symbols were selected in such a way to meet the following conditions:

- (i) there is enough information at the symbol level to provide an immediate indication of the grid orientation;
- (ii) the symbol recognition procedure is invariant to position, and orientation;
- (iii) the symbols have a certain peculiarity so that other objects in the scene will not be mistaken for encoding symbols.

The shape of the four code symbols for a PRA over  $GF(4)$  embossed on object's surface



"0"



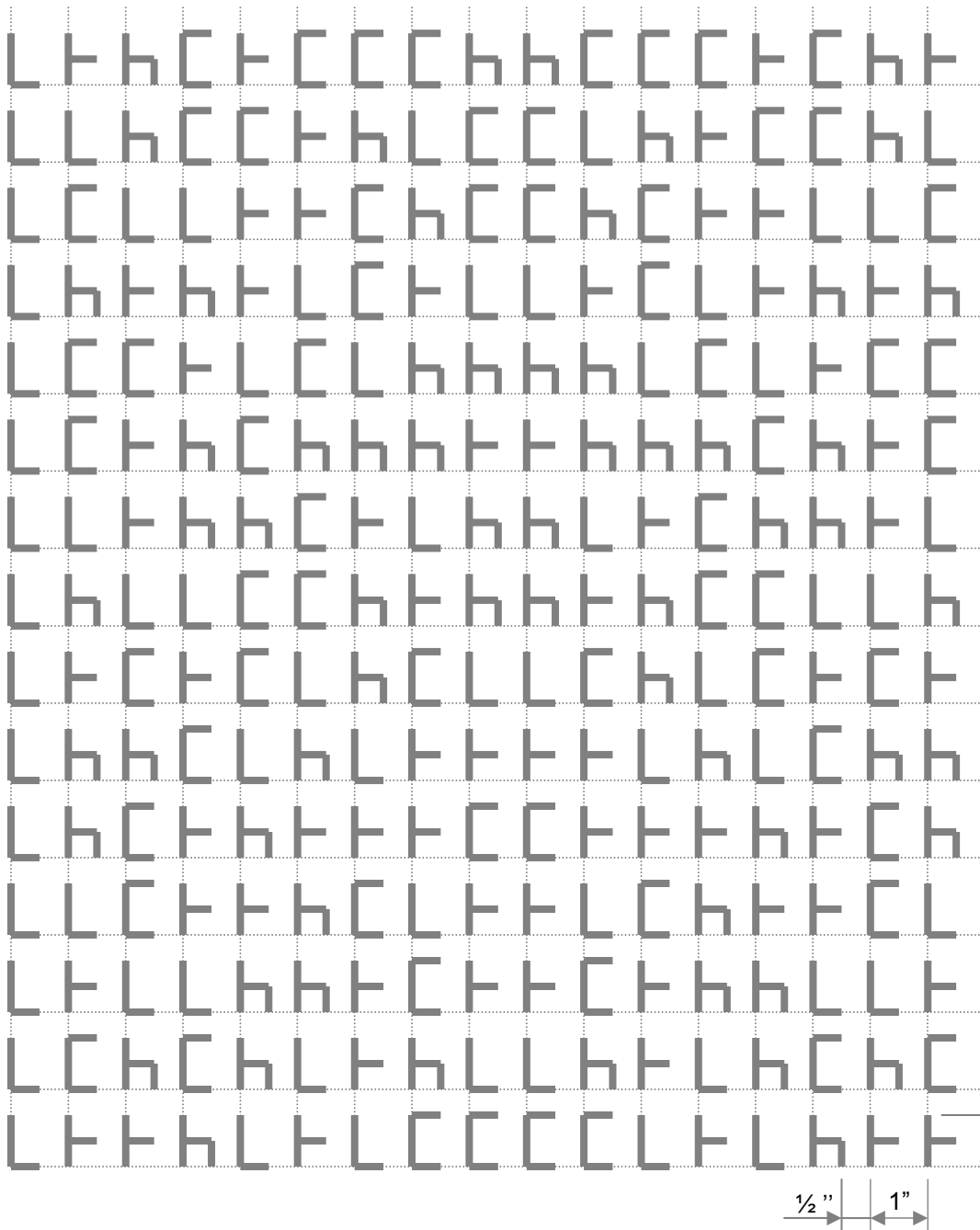
"1"



"A"

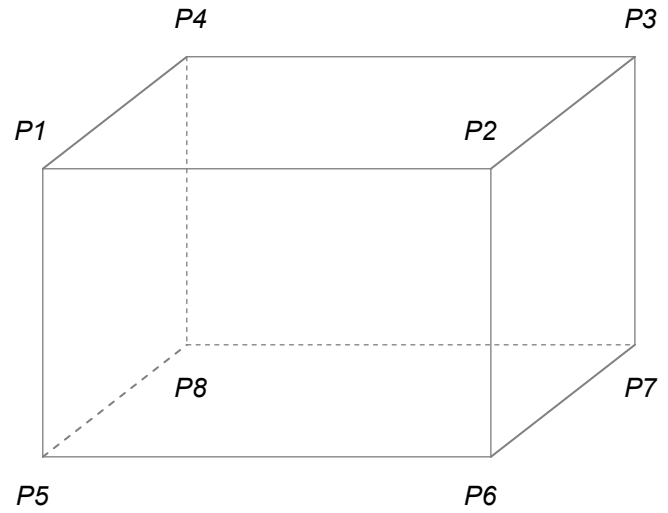
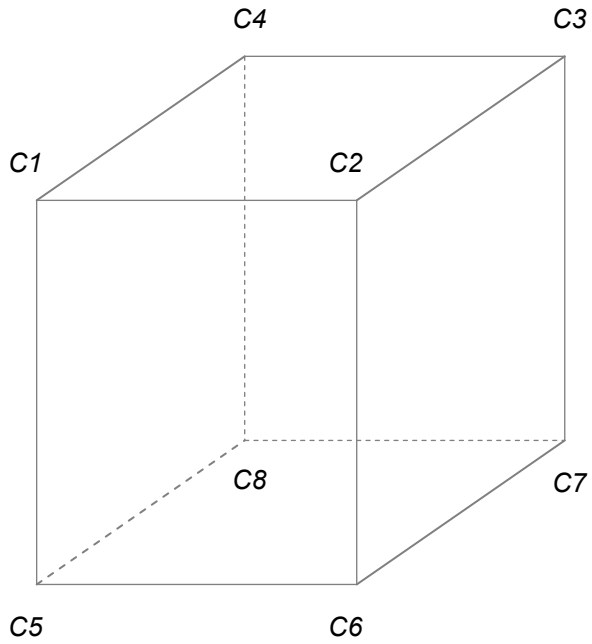


"A<sup>2</sup>"

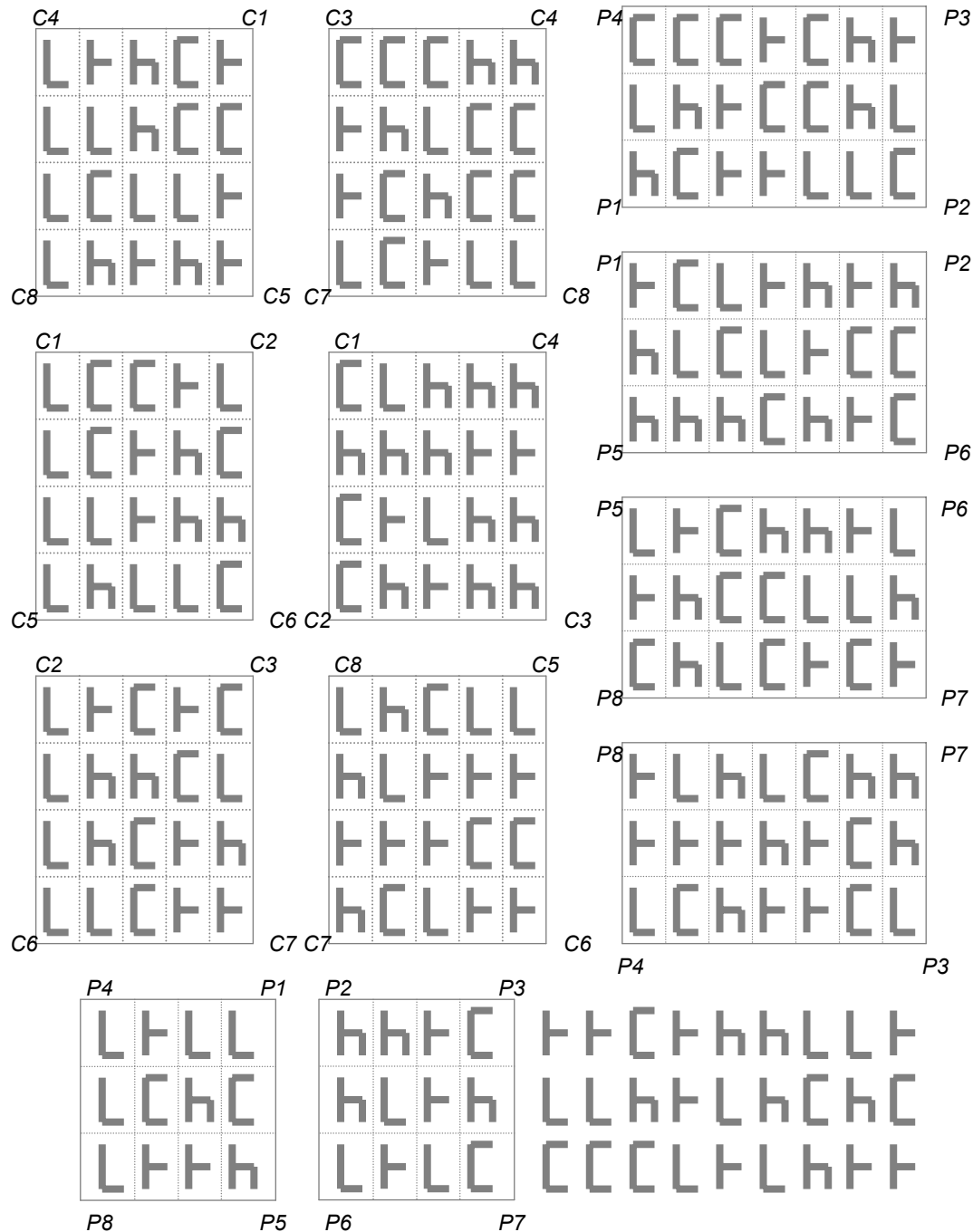


Physical layout of the 15-by-17 PRA with the code elements represented by four embossing symbols. The symbols are set 25.4 mm (1 inch) apart in the horizontal direction and 31.75 mm (1¼ inch) apart in the horizontal direction, providing a clear space of 12.7 mm (½ inch) between symbols in both directions.

(from [E.M. Petriu, S.K.S. Yeung, S.R. Das, A.M. Cretu, H.J.W. Spoelder, "Robotic Tactile Recognition of Pseudorandom Encoded Objects, IEEE Trans. Instrum. Meas., Vol.53, No.5, pp.1425-1432, 2004.]



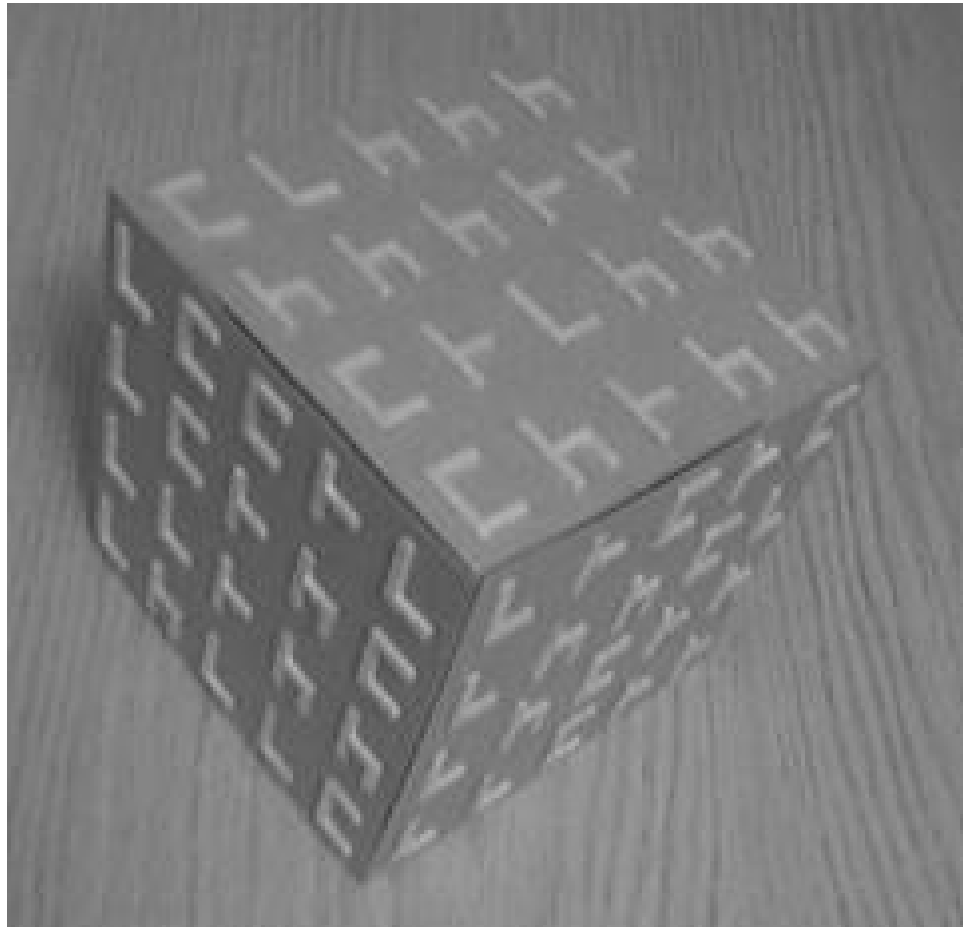
The vertex labeled models of two simple 3D objects



Mapping the embossed PRBA on the surfaces of the two 3D objects

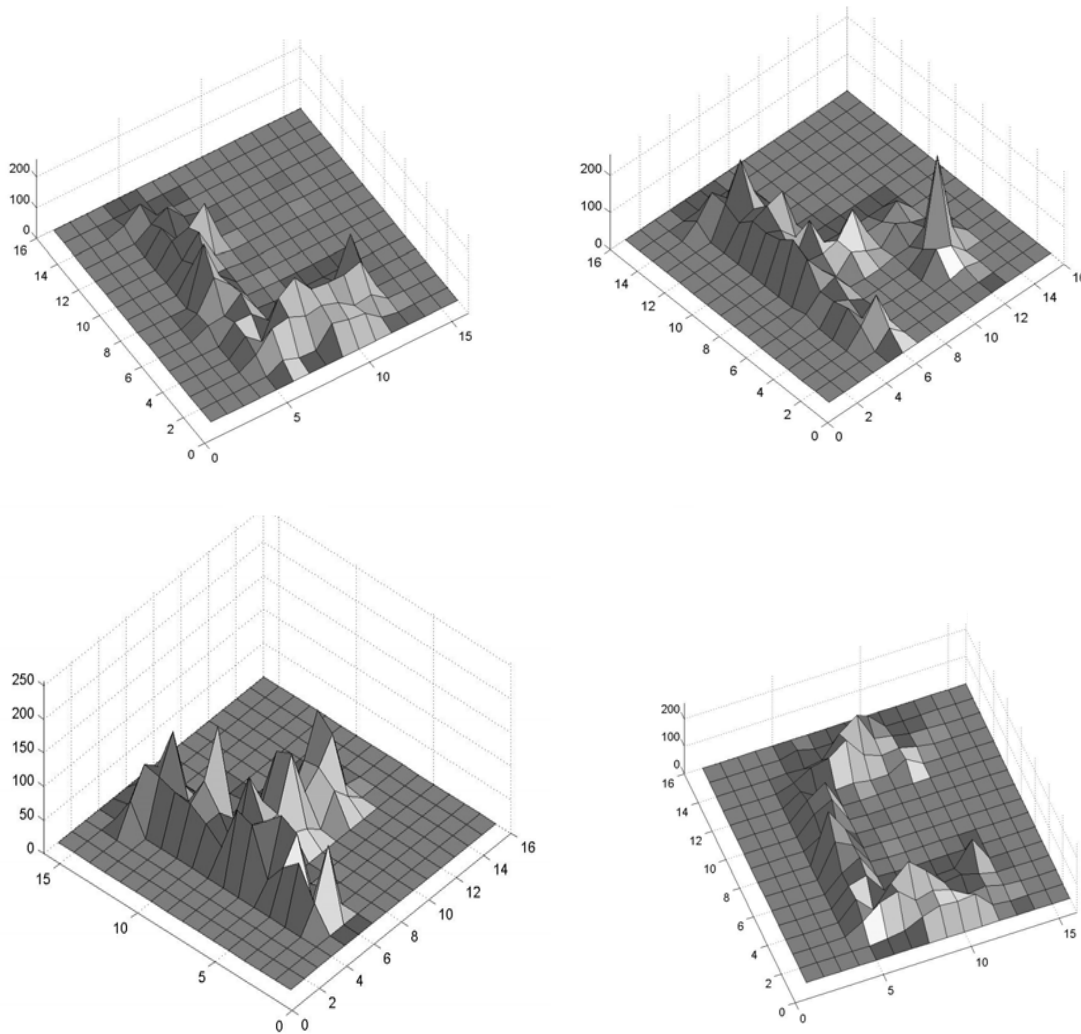
(from [E.M. Petriu, S.K.S. Yeung, S.R. Das, A.M. Cretu, H.J.W. Spoelder, "Robotic Tactile Recognition of Pseudorandom Encoded Objects, IEEE Trans. Instrum. Meas., Vol.53, No.5, pp.1425-1432, 2004.])





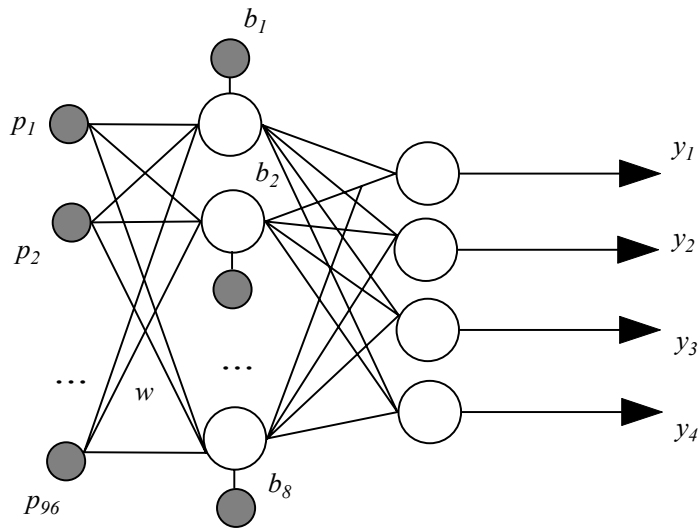
The PRA encoded cube.

(from [E.M. Petriu, S.K.S. Yeung, S.R. Das, A.M. Cretu, H.J.W. Spoelder, "Robotic Tactile Recognition of Pseudorandom Encoded Objects, IEEE Trans. Instrum. Meas., Vol.53, No.5, pp.1425-1432, 2004.])

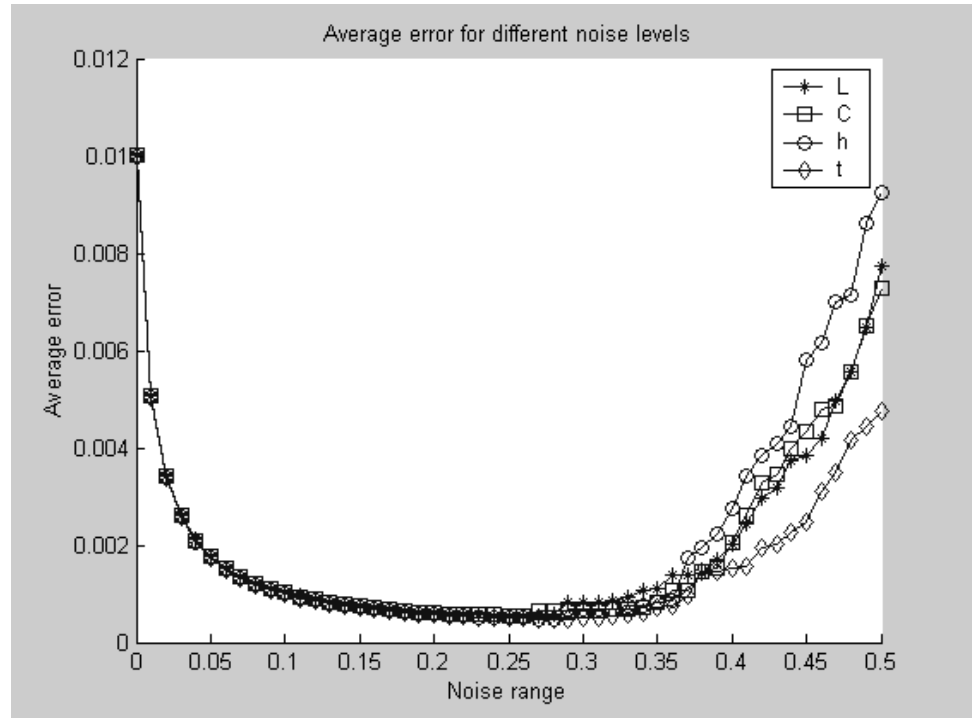


Tactile images of the four GF(4) symbols. The two rectangular axes on the horizontal plane in each image indicate the 2D node coordinates of the 16-by-16 tactile image. One unit on the vertical axis corresponds to 0.015875 mm (0.01/16 inch).

(from [E.M. Petriu, S.K.S. Yeung, S.R. Das, A.M. Cretu, H.J.W. Spoelder, "Robotic Tactile Recognition of Pseudorandom Encoded Objects, IEEE Trans. Instrum. Meas., Vol.53, No.5, pp.1425-1432, 2004.]

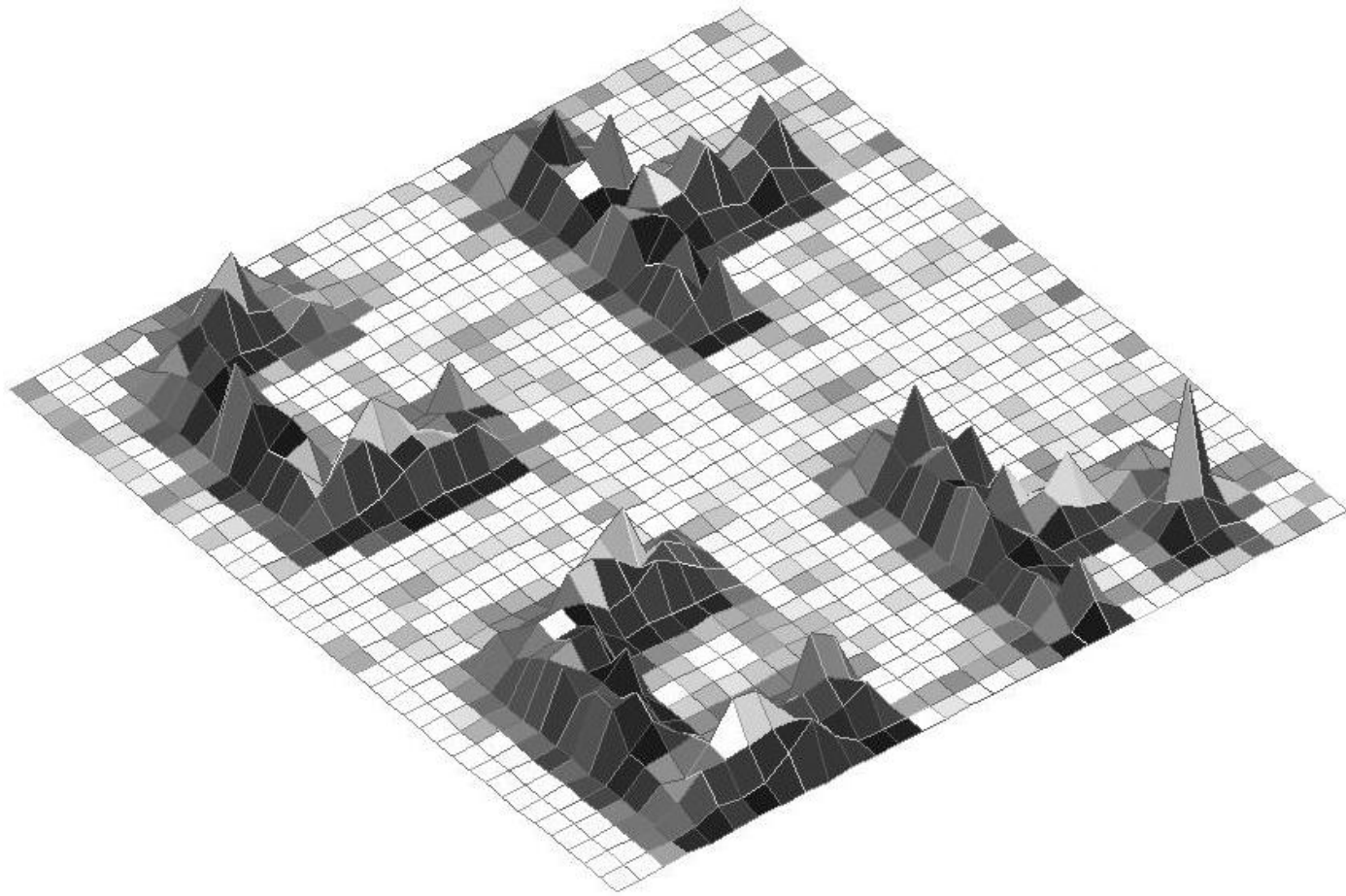


Two-layer feedforward NN architecture for the classification of the four GF(4) symbols.



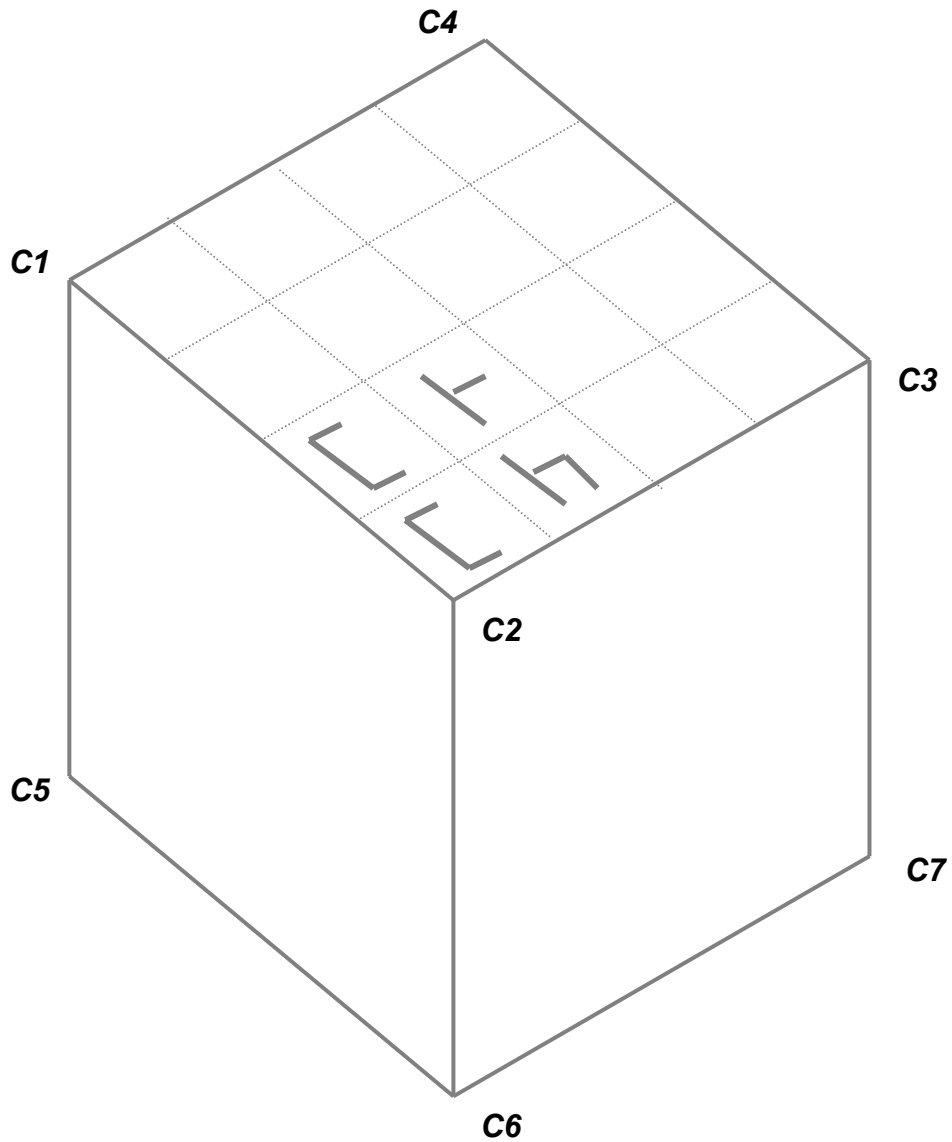
Average error rate for noise ranging between 0 and 0.5

(from [E.M. Petriu, S.K.S. Yeung, S.R. Das, A.M. Cretu, H.J.W. Spoelder, "Robotic Tactile Recognition of Pseudorandom Encoded Objects, IEEE Trans. Instrum. Meas., Vol.53, No.5, pp.1425-1432, 2004.]



Composite tactile image of four symbols  
on an encoded object surface

(from [E.M. Petriu, S.K.S. Yeung, S.R. Das, A.M. Cretu, H.J.W. Spoelder, "Robotic Tactile Recognition of Pseudorandom Encoded Objects, IEEE Trans. Instrum. Meas., Vol.53, No.5, pp.1425-1432, 2004.] )

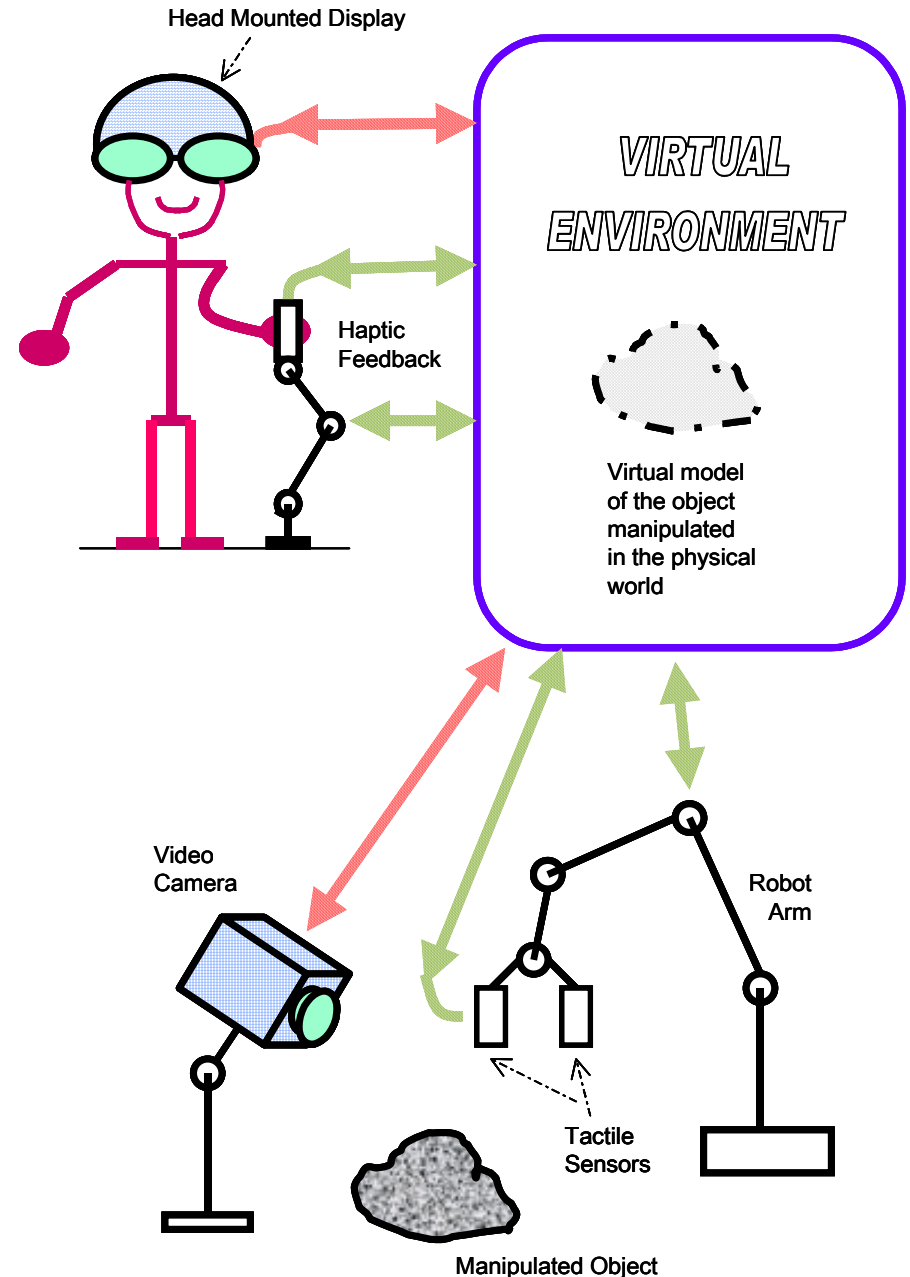


The four tactile recovered symbols are recognized, And their location is unequivocally identified on the face of one of the 3D objects, using the PRA window property.

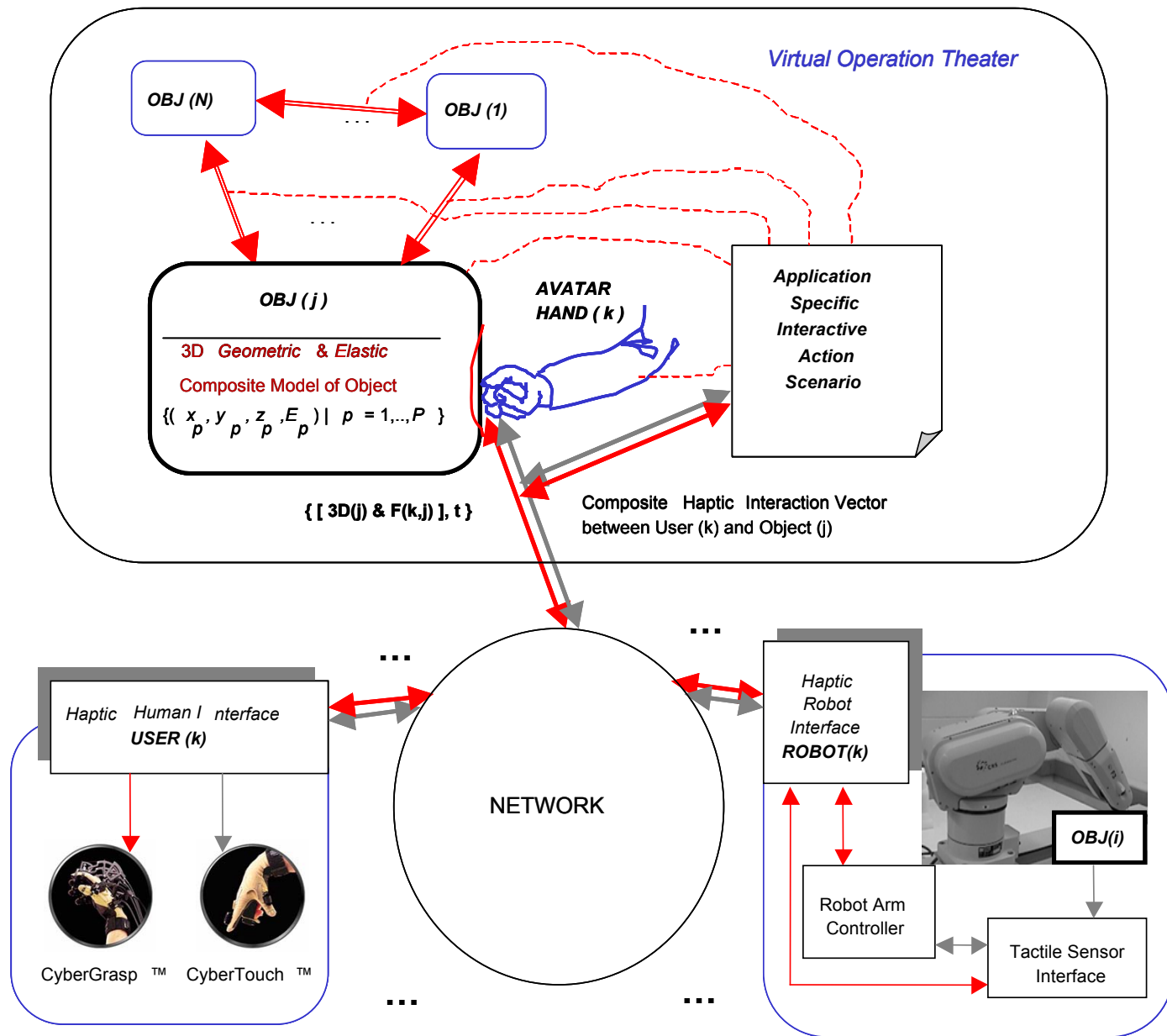
(from [E.M. Petriu, S.K.S. Yeung, S.R. Das, A.M. Cretu, H.J.W. Spoelder, "Robotic Tactile Recognition of Pseudorandom Encoded Objects, IEEE Trans. Instrum. Meas., Vol.53, No.5, pp.1425-1432, 2004.]

## Sensor Enabled Robotic Telemanipulation

*Robotic dexterous manipulation* is an object-oriented act which requires not only specialized *robotic hands with articulated fingers* but also *tactile, force and kinesthetic sensors* for the precise control of the forces and motions exerted on the manipulated object. As fully autonomous robotic dexterous manipulation is impractical in changing and unstructured environments, an alternative approach is to *combine the low-level robot computer control with the higher-level perception and task planning abilities of a human operator* equipped with adequate *human computer interfaces* (HCI).



- ❑ Telesmanipulation systems should have a bilateral architecture that allows a *human operator* to connect in a transparent manner to a remote robotic manipulator.
  
- ❑ *Human Computer Interfaces* (HCI) should provide easily perceivable and *task-related sensory displays (monitors)* which fit naturally the perception capabilities of the human operator.
  
- ❑ The potential of the emergent haptic perception technologies is significant for *applications* requiring object telesmanipulation such as: (i) robot-assisted handling of materials in industry, hazardous environments, high risk security operations, or difficult to reach environments, (ii) telelearning in hands-on virtual laboratory environments for science and arts, (iii) telemedicine and medical training simulators.

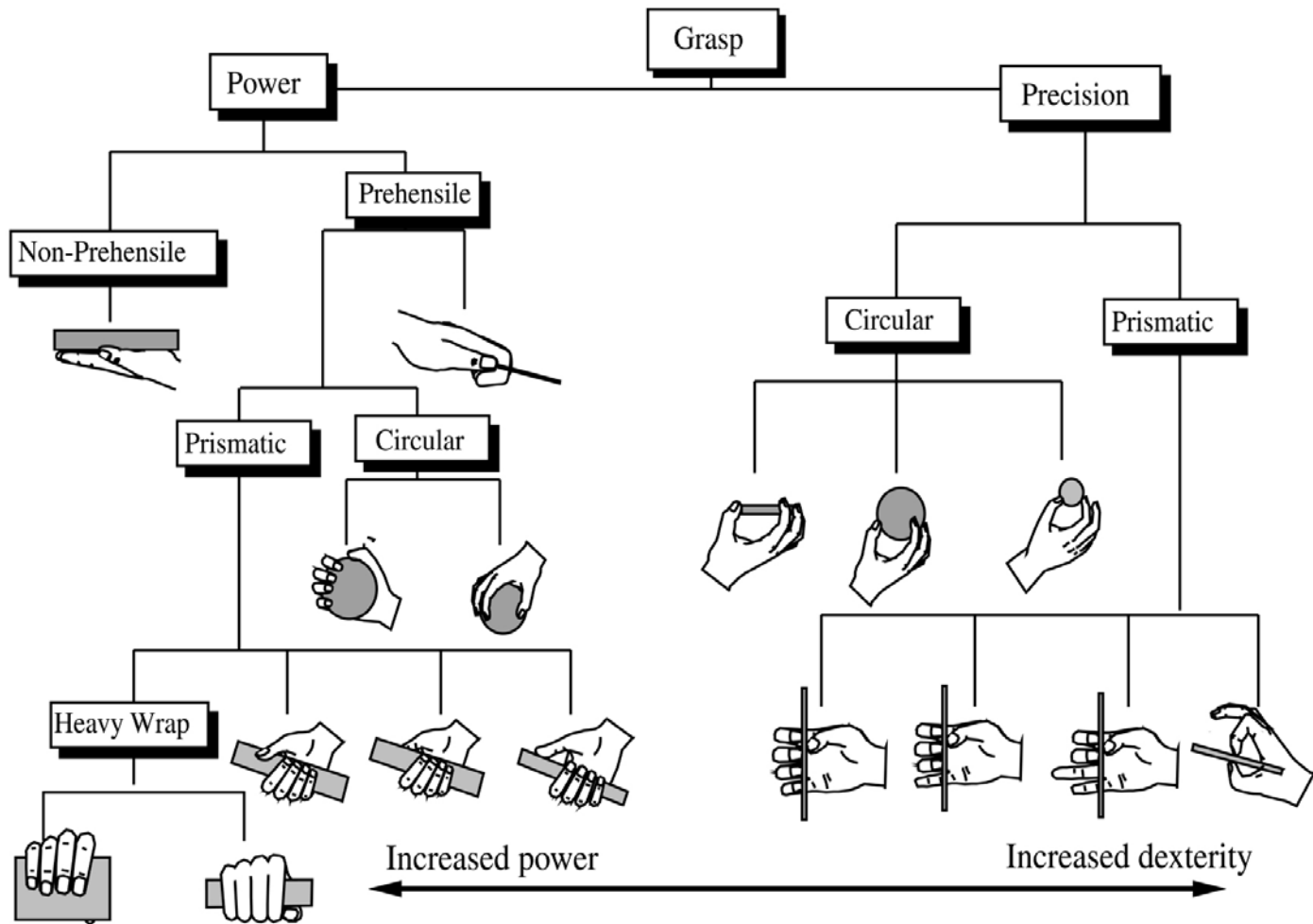


**Interactive Model-Based Hapto-Visual Teleoperation** - a human operator equipped with haptic HCI can telemanipulate physical objects with the help of a robotic equipped with haptic sensors.

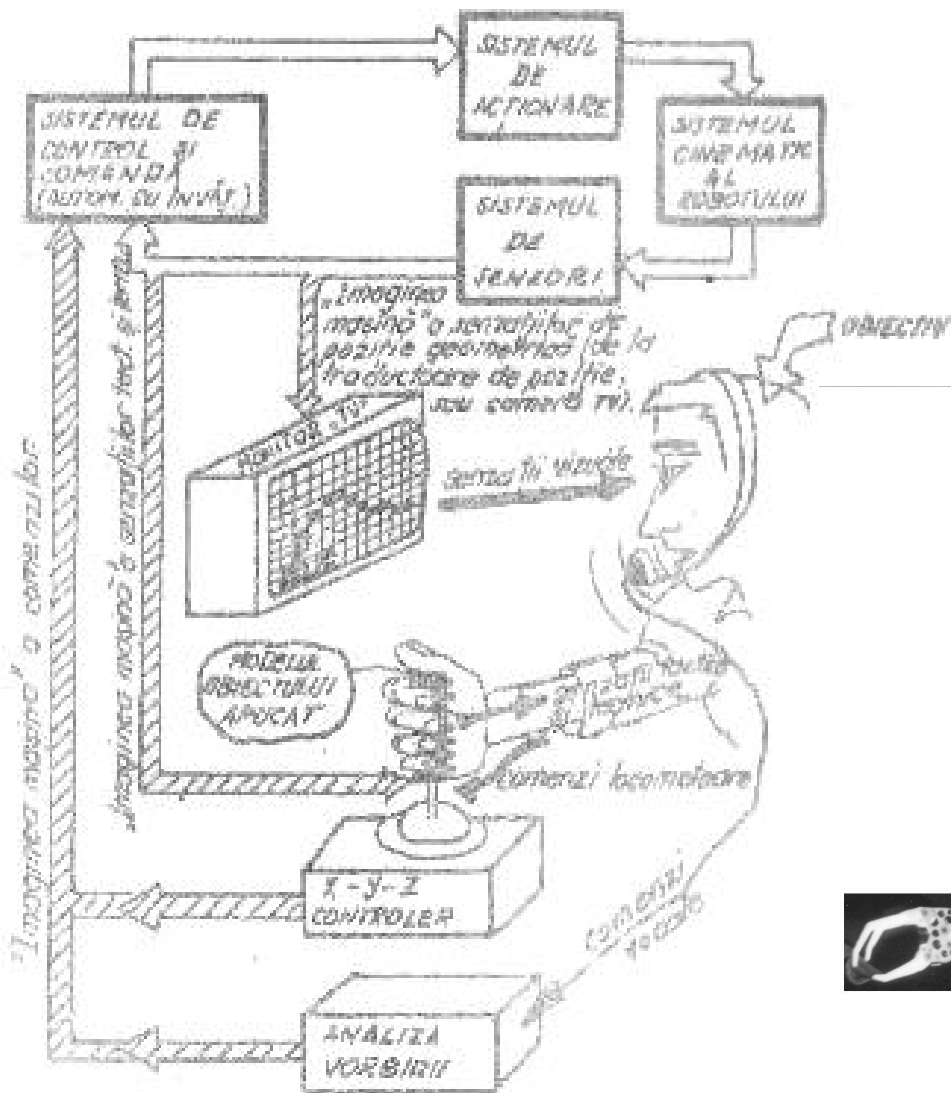


## Haptic Human Interfaces

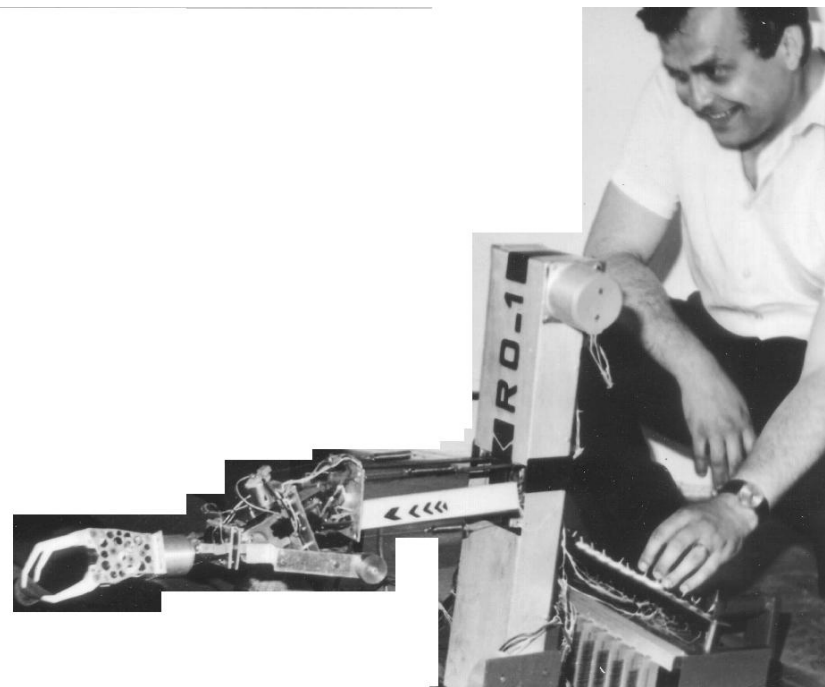
- These interfaces should allow the human operator to experience natural-like, *conformal to the reality*, feeling of geometric profile, force, texture, elasticity temperature, etc.
- These interfaces should have easily perceivable and *sensor-transparent information displays* (monitors) in such a way to offer a 1:1 mapping of the corresponding human sensory medium.



Human grasping configurations (from [Burdea & Coiffet 2003])

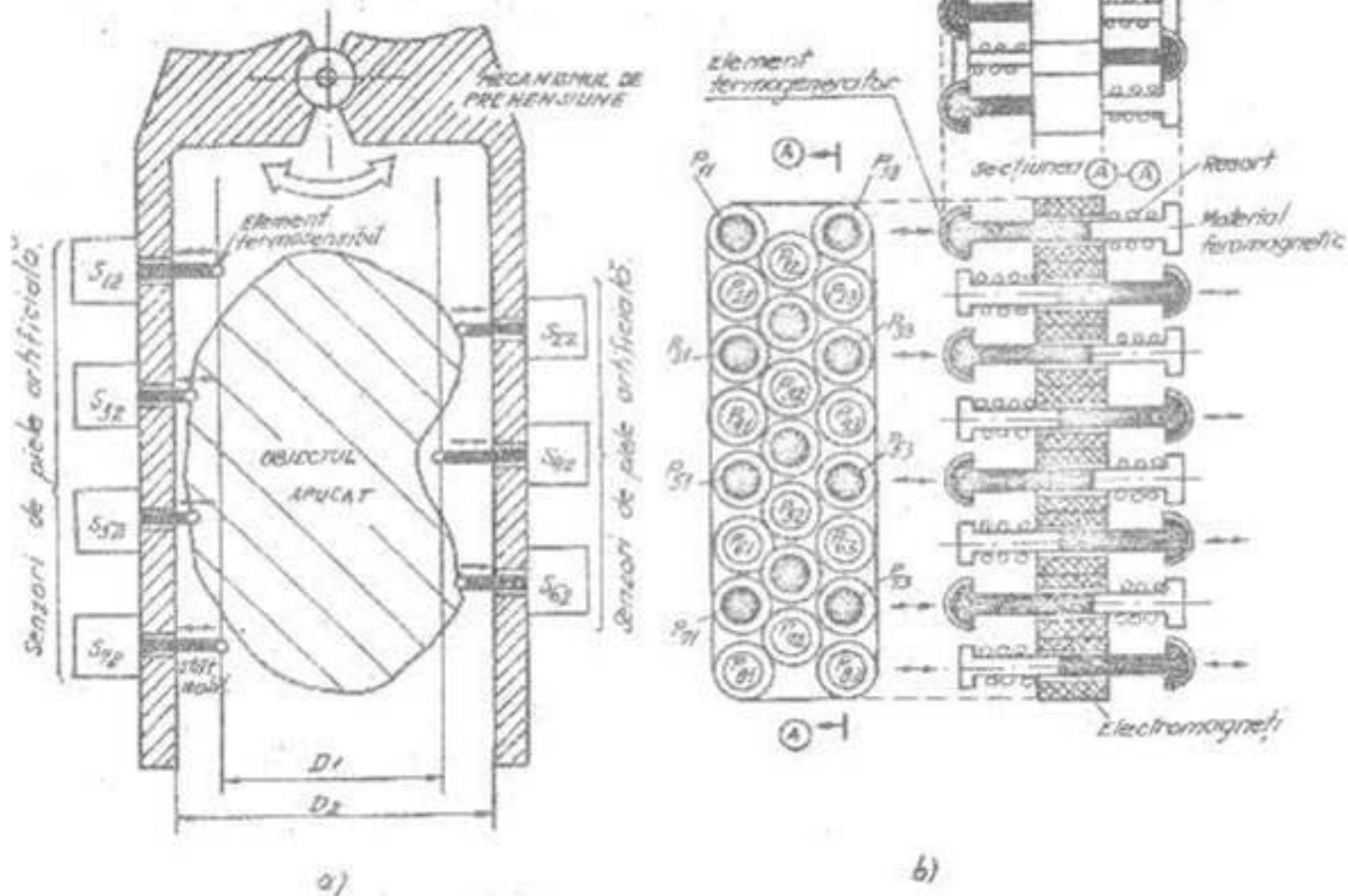


System architecture



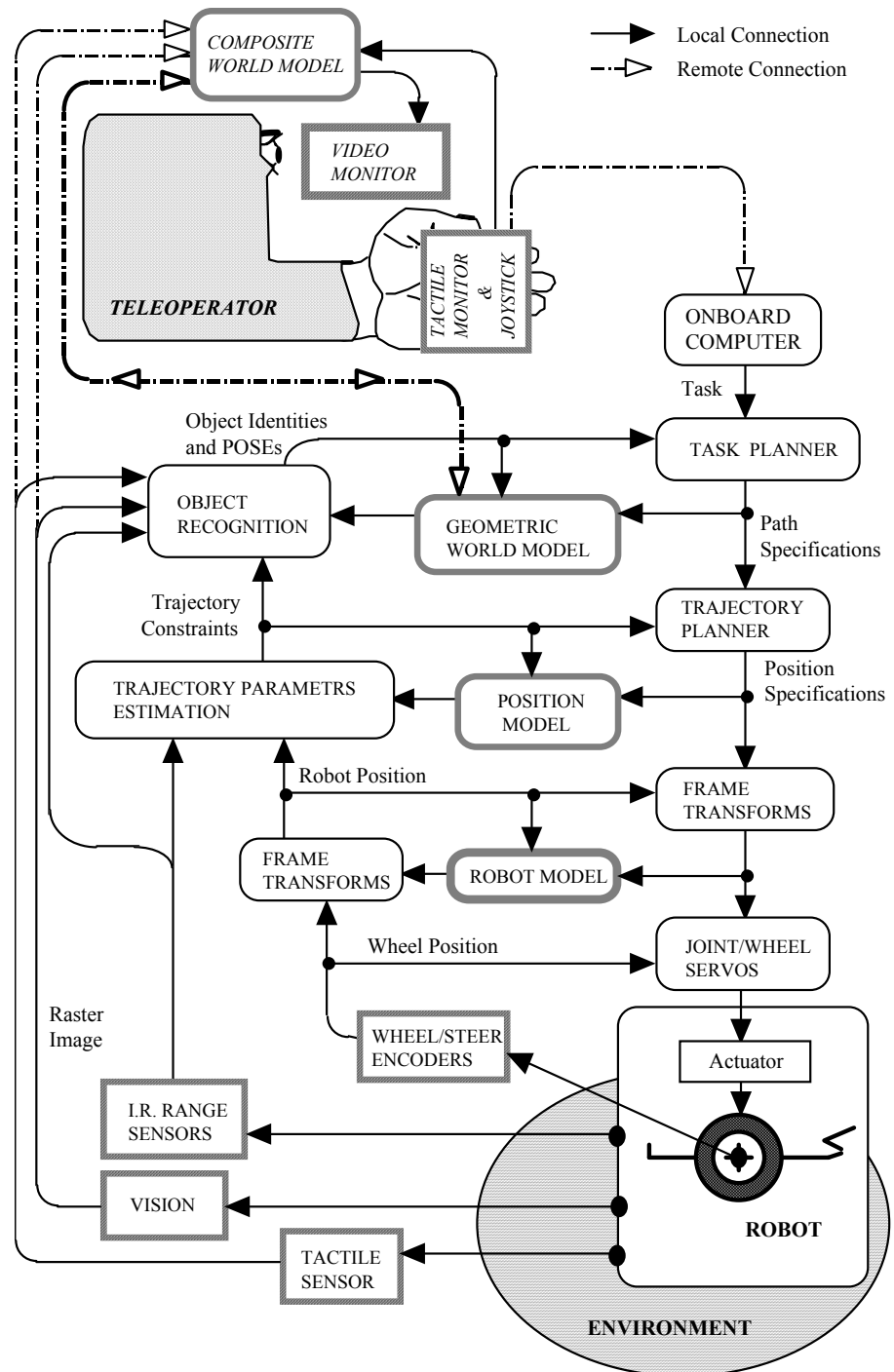
Robot arm with tendon driven compliant wrist

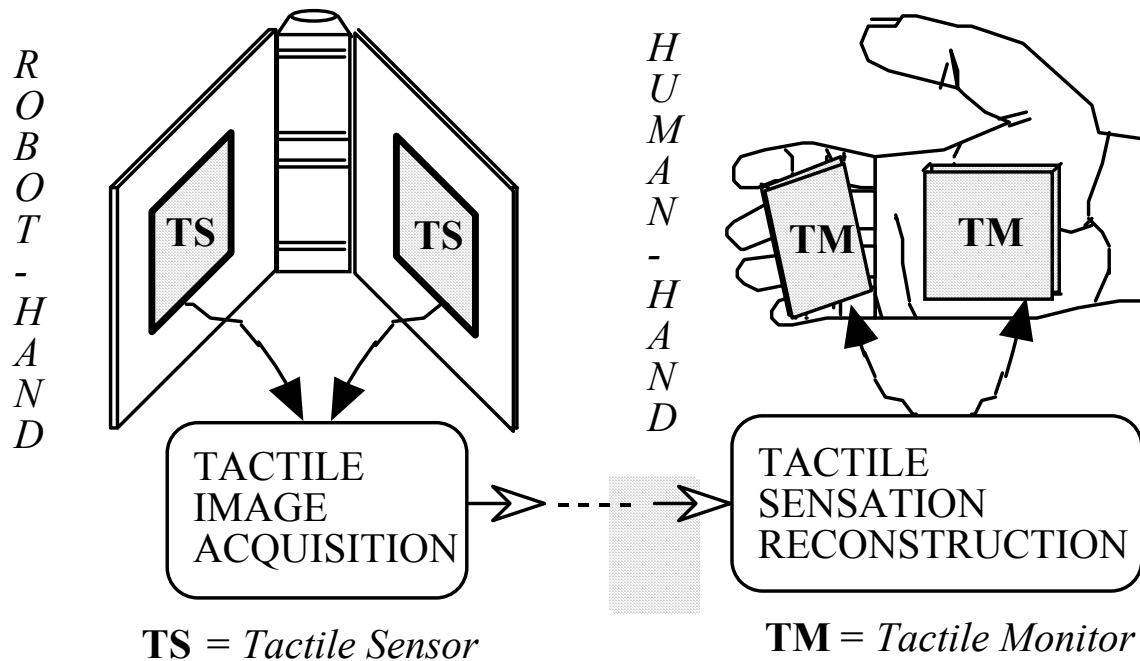
**Video and Haptic Telerobotic System** (from [E.M. Petriu, D.C. Petriu, V. Cretu, "Control System for an Interactive Programmable Robot," *Proc. CNETAC Nat. Conf. Electronics, Telecommunications, Control, and Computers*, pp. 227-235, Bucharest, Romania, Nov. 1982]).



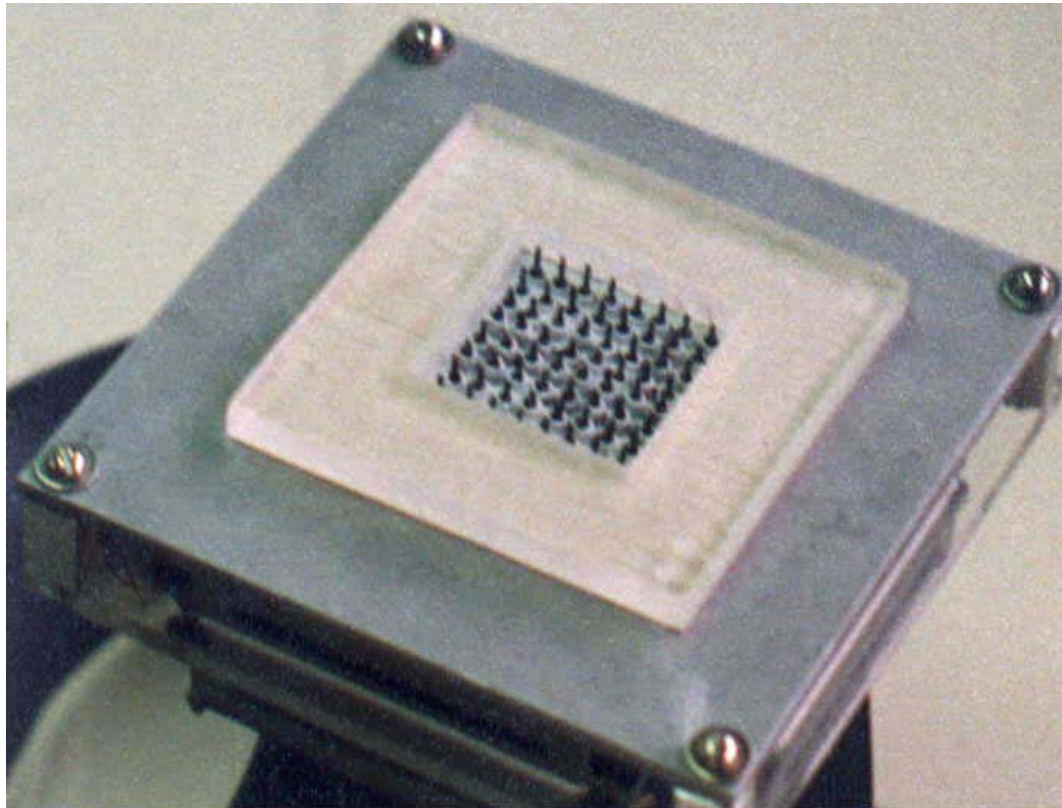
**Video and Haptic Telerobotic System:** (a) the tactile probe , and (b) the tactile human feedback (from [E.M. Petriu, D.C. Petriu, V. Cretu, "Control System for an Interactive Programmable Robot," *Proc. CNETAC Nat. Conf. Electronics, Telecommunications, Control, and Computers*, pp. 227-235, Bucharest, Romania, Nov. 1982.])

# Model-based telepresence control of a robot (early 90s)

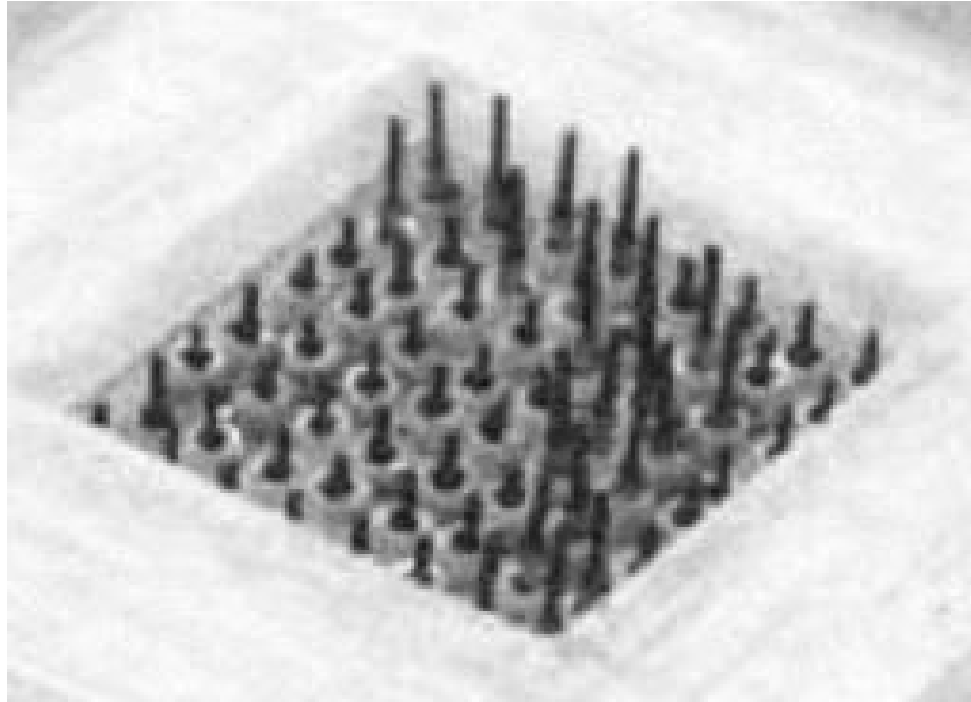




A **tactile human feedback interface** placed on the operator's palm allows the human teleoperator to virtually feel by touch the object profile measured by the tactile sensors placed in the jaws of the robot gripper (from [E.M. Petriu, W.S. McMath, "Tactile Operator Interface for Semi-autonomous Robotic Applications," *Proc.Int. Symposium on Artificial Intell. Robotics Automat. in Space, i-SAIRS'92*, pp.77-82, Toulouse, France, 1992.])

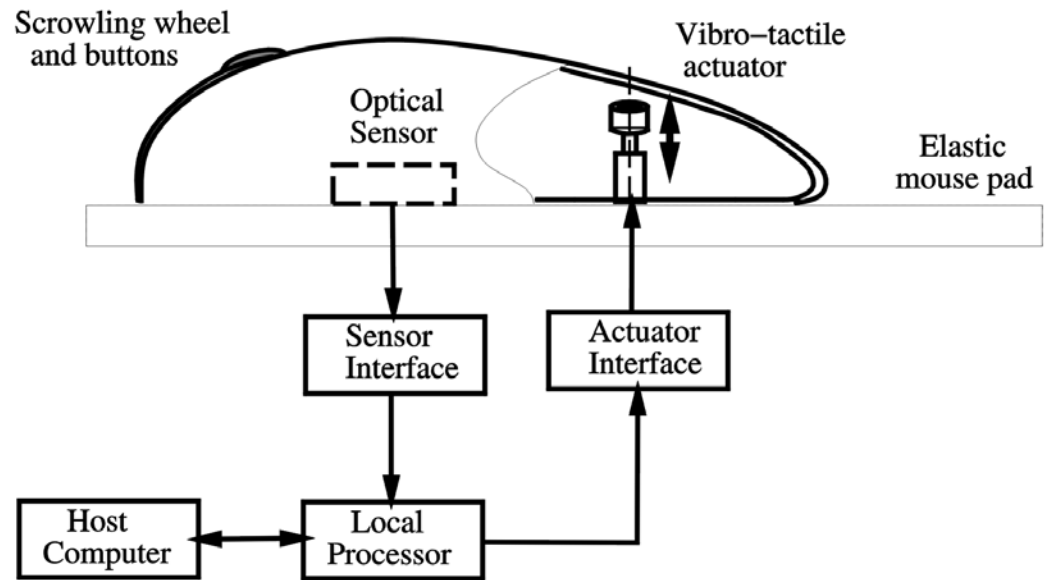


**Tactile human feedback interface** developed for the *Canadian Space Agency* in the early 90s. It consists of an 8-by-8 array of electromagnetic vibrotactile stimulators. The active area 6.5 cm<sup>2</sup> is the same as that of the tactile sensor. (from [E.M. Petriu, W.S. McMath, "Tactile Operator Interface for Semi-autonomous Robotic Applications," *Proc.Int. Symposium on Artificial Intell. Robotics Automat. in Space, i-SAIRS'92*, pp.77-82, Toulouse, France, 1992.])



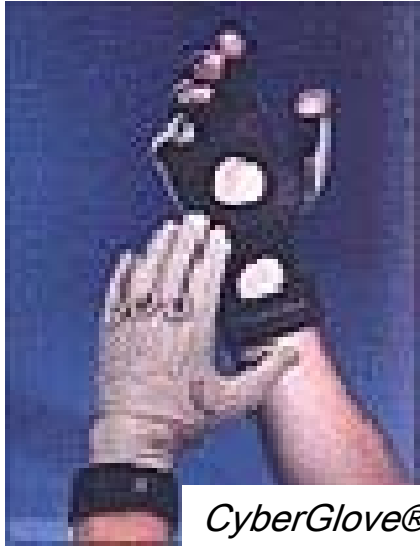
Each stimulator corresponds to a 2-by-2 window in the tactile sensor array. The vibrotactile stimulators are used as binary devices that are activated when at least two of the corresponding *taxe/s* (tactile elements) in the tactile sensor array window are "on". The figure shows a curved edge tactile feedback .





**Logitech iFeel Mouse (0-125 Hz).**

*Immersionn\_3D Interaction* <<http://www.immersion.com/>>



*CyberGlove®*



*CyberTouch™*



*CyberGrasp™*



*CyberForce®*

## Performance comparison of various sensing gloves [Burdea & Coiffet 2003]

**Table 2.3** Performance comparison of various sensing gloves

<b>Specs</b>	<b>Pinch Glove</b>	<b>5DT Glove</b>	<b>DidjiGlove</b>	<b>CyberGlove</b>
<b>Number Sensors</b>	7/glove (two gloves)	5 or 14 /glove (one glove)	10/glove (two gloves)	18 or 22/glove (one glove)
<b>Sensor type</b>	electrical	fiberoptic	capacitive	strain gauge
<b>Records /sec</b>	??	100 (5DT 5W) 200 (5DT 5)	70	150 (unfiltered) 112 (filtered)
<b>Sensor resolution</b>	1 bit (two points)	8 bit (256 points)	10 bit (1,024 points)	0.5°
<b>Comm. rates</b>	wired (19.2 kb)	wireless (9.600 kb) wired (19.2 kb)	wired (19.2 kb)	wired (115 kb)
<b>Wrist sensors</b>	none	pitch (5DT 5 model)	none	pitch and yaw



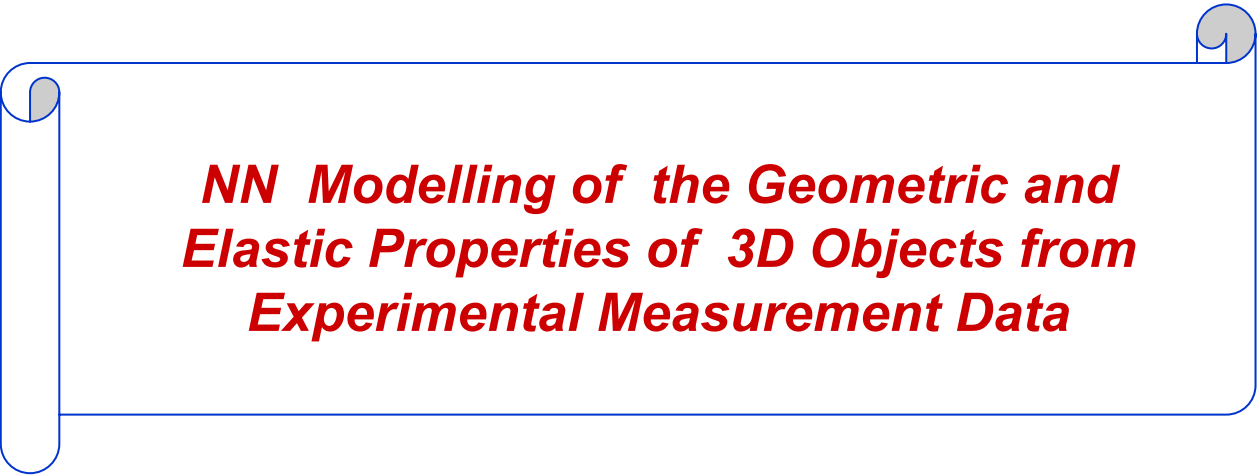
6 individually  
controlled  
vibrotactile  
actuators

0-125 Hz frequency;  
1.2 N amplitude at 125 Hz.

**CyberTouch Glove (Virtex)** (from [Burdea & Coiffet 2003])



Commercial “**Virtual Hand Toolkit for CyberGlove/Grasp**”  
providing the kinesthetic human feedback interface



***NN Modelling of the Geometric and  
Elastic Properties of 3D Objects from  
Experimental Measurement Data***

*Model-based approach*, based on the kinematics and dynamics of the object handled with the fingertips, provides a convenient representation of the dexterous manipulation.

Quoting Salisbury, Conti, and Barbagli's recent survey of haptic rendering: *"improved accuracy and richness in object modeling and haptic rendering will require advances in our understanding of how to represent and render psychophysically and cognitively germane attributes of objects, as well as algorithms and perhaps specialty hardware (such as haptic or physics engines) to perform real-time computations"*.

---

K. Salisbury, F. Conti, F. Barbagli, "Haptic Rendering: Introductory Concepts," *IEEE Computer Graphics and Applications*, Vol. 24, No. 2, pp. 24 – 32, 2004.

**Modelling** allows to *simulate the behavior of a system* for a variety of initial conditions, excitations and systems configurations

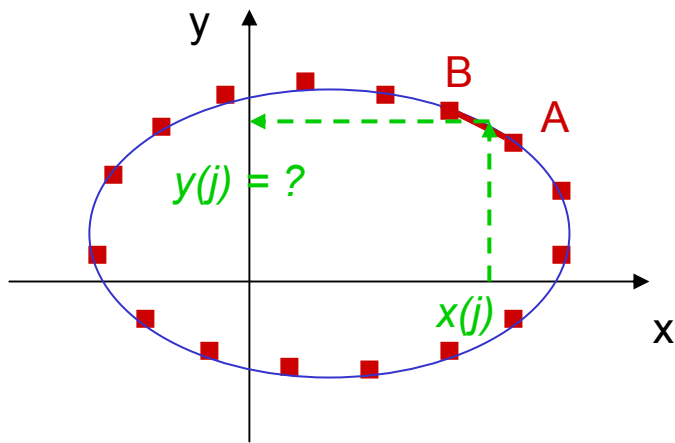
- ★ The ***quality and the degree of the approximation*** of the model can be determined only by a validation against experimental measurements.
- ★ The ***convenience*** of the model means that it is capable of performing extensive parametric studies, in which independent parameters describing the model can be varied over a specified range in order to gain a global understanding of the response.

---

E.M. Petriu, "Neural Networks for Measurement and Instrumentation in Virtual Environments," in *Neural Networks for Instrumentation, Measurement and Related Industrial Applications*, S. Ablameyko, L. Goras, M. Gori, V. Piuri - Eds.), NATO Science Series, Series III: Computer and System Sciences Vol. 185, pp.273-290, IOS Press, 2003



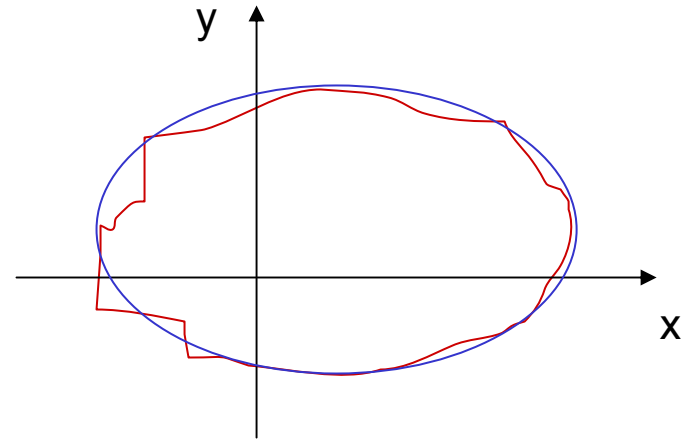
## Discret vs. Continuous Modelling of Physical Objects and Processes



### DISCREET MODEL

- *sampling* => INTERPOLATION COST

$$y(j) = y(A) + \frac{[x(j) - x(B)] \cdot [y(B) - y(A)]}{[x(A) - x(B)]}$$



### CONTINUOUS MODEL

- *NO sampling* =>  
NO INTERPOLATION COST

## Analog Computer vs. Neural Network Modelling of Continuous Physical Objects and Processes



- ❑ Both the Analog Computers and the Neural Networks are *continuous modelling devices*.
- ❑ The Analog Computer (AC) allows to *solve the linear or nonlinear differential and/or integral equations representing mathematical model* of a given physical process. The coefficients of these equations must be exactly known as they are used to program/adjust the coefficient-potentiometers of the AC's computing-elements (OpAmps). The AC doesn't follow a sequential computation, all its computing elements perform simultaneously and continuously. An interesting note, "because of the difficulties inherent in analog differentiation the [differential] equation is rearranged so that it can solved by integration rather than differentiation." [A.S. Jackson, *Analog Computation*, McGraw-Hill Book Co., 1960].

- The Neural Network (NN) doesn't require a prior mathematical model. A *learning algorithm* is used to adjust, sequentially by trial and error during the learning phase, the synaptic-weights/coefficient-potentiometers of the neurons/computing-elements.

Similarly to the analog computer, a NN doesn't follow a sequential computation algorithm, all its neurons performing simultaneously and continuously. The neurons are also integrative-type processing elements.

**Recovery of the elastic material properties** requires touching each point of interest on the explored object surface and then conducting a strain-stress relation measurement on each point.

**Tactile probing is a time consuming Sequential operation**

 *Find fast sampling procedures able to minimize the number of the sampling points by selecting only those points that are relevant to the elastic characteristics.* 

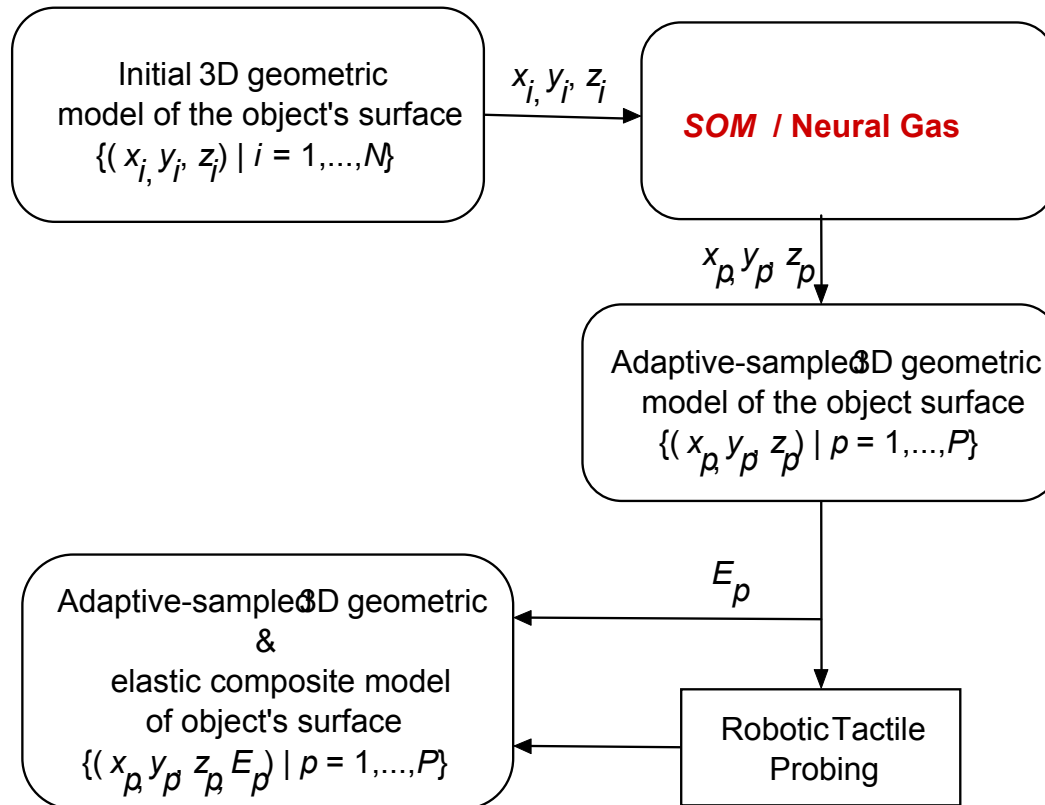
***non-uniform adaptive sampling algorithm of the object's surface,*** which exploits the SOM (*self-organizing map*) ability to find optimal finite quantization of the input space.

The elastic behaviour at any given point  $(x_p, y_p, z_p)$  on the object surface is described by the Hooke's law:

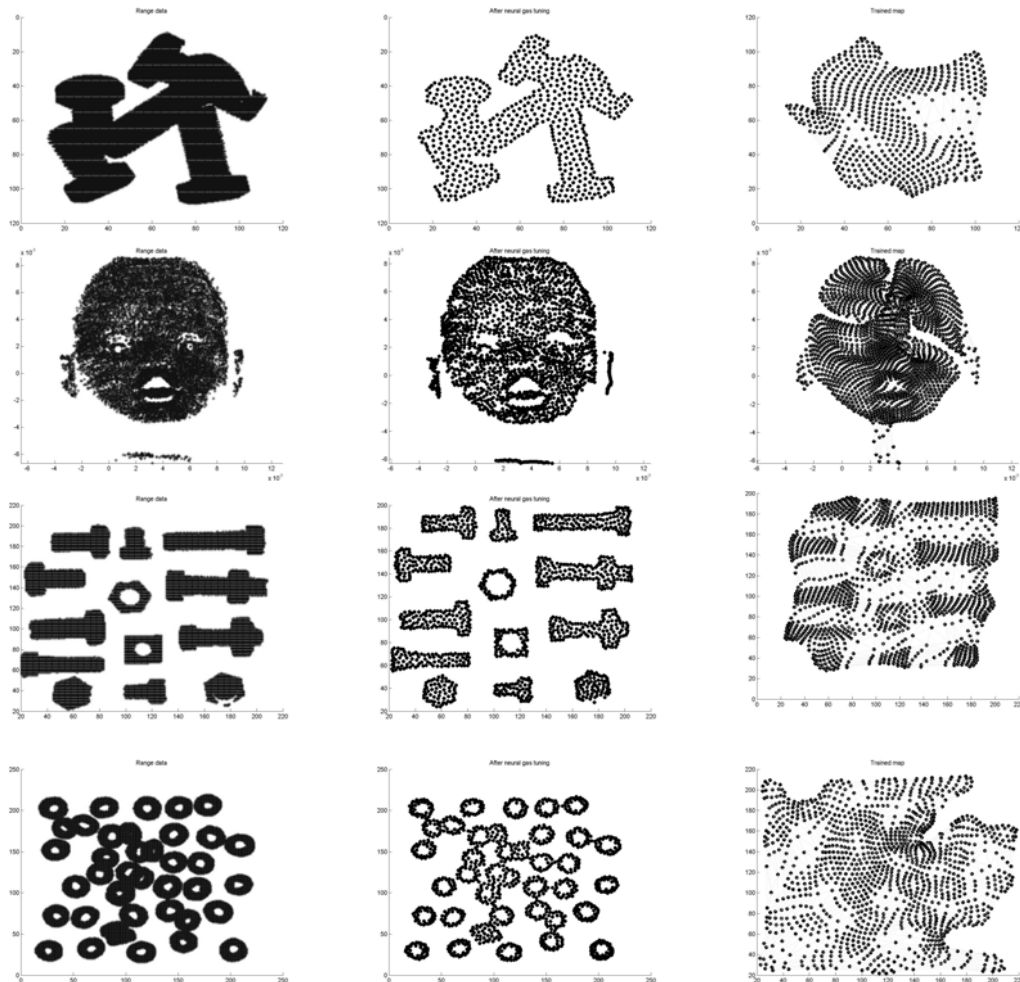
$$\begin{cases} \sigma_p = E_p \cdot \varepsilon_p & \text{if } 0 \leq \varepsilon_p \leq \varepsilon_{p \max} \\ \sigma_p = \sigma_{p \max} & \text{if } \varepsilon_{p \max} < \varepsilon_p \end{cases}$$

where  $E_p$  is the modulus of elasticity,  $\sigma_p$  is the stress, and  $\varepsilon_p$  is the strain on the normal direction.

# Adaptive Sampling Control of the Robotic Tactile Probing of Elastic Properties of 3D Object Surfaces

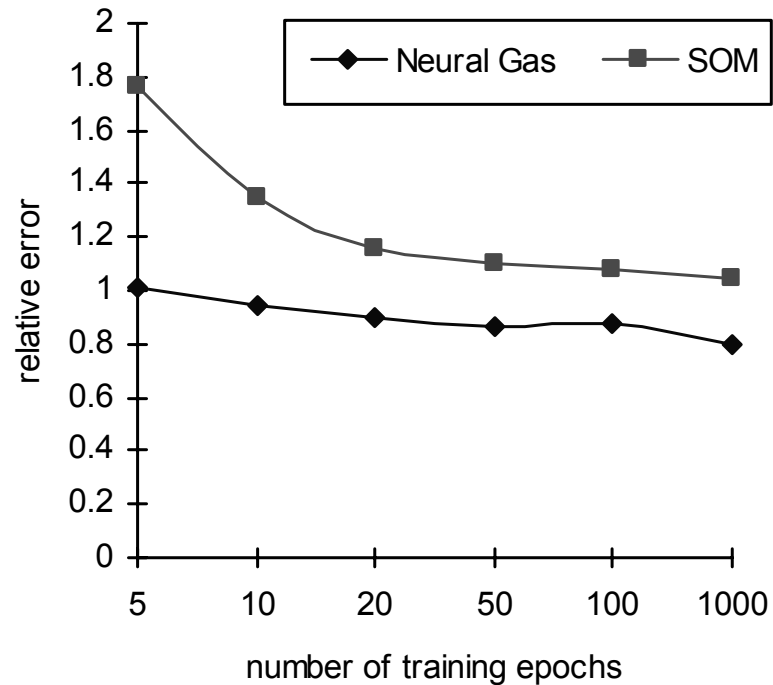


- ❑ **SOM** (Self Organizing Map) and **Neural Gas** NN architectures are both used to build compressed model of the 3D object originally defined as a point-cloud.
- ❑ The weight vector will consist of the 3D coordinates of the object's points.
- ❑ During the learning procedure, the model will contract asymptotically towards the points in the input space, respecting their density and thus taking the shape of the object encoded in the point-cloud.
- ❑ Data point-clouds obtained with a range scanner are used to train the network. Normalization is employed to remove redundant information from a data set, by a linear rescaling of the input vectors such that their variance is 1.
- ❑ In order to evaluate the quality of the models, a straightforward measure of the precision is used. The precision is estimated as the average distance between each data vector and its winning neuron .



## Qualitative comparison between the Neural Gas and the SOM adaptive sampled models.

- The map sizes are equal for both networks.
- The *first column* represents the original point-cloud,
- The *second column* represents the Neural Gas model.
- The *third column* represents the SOM model.



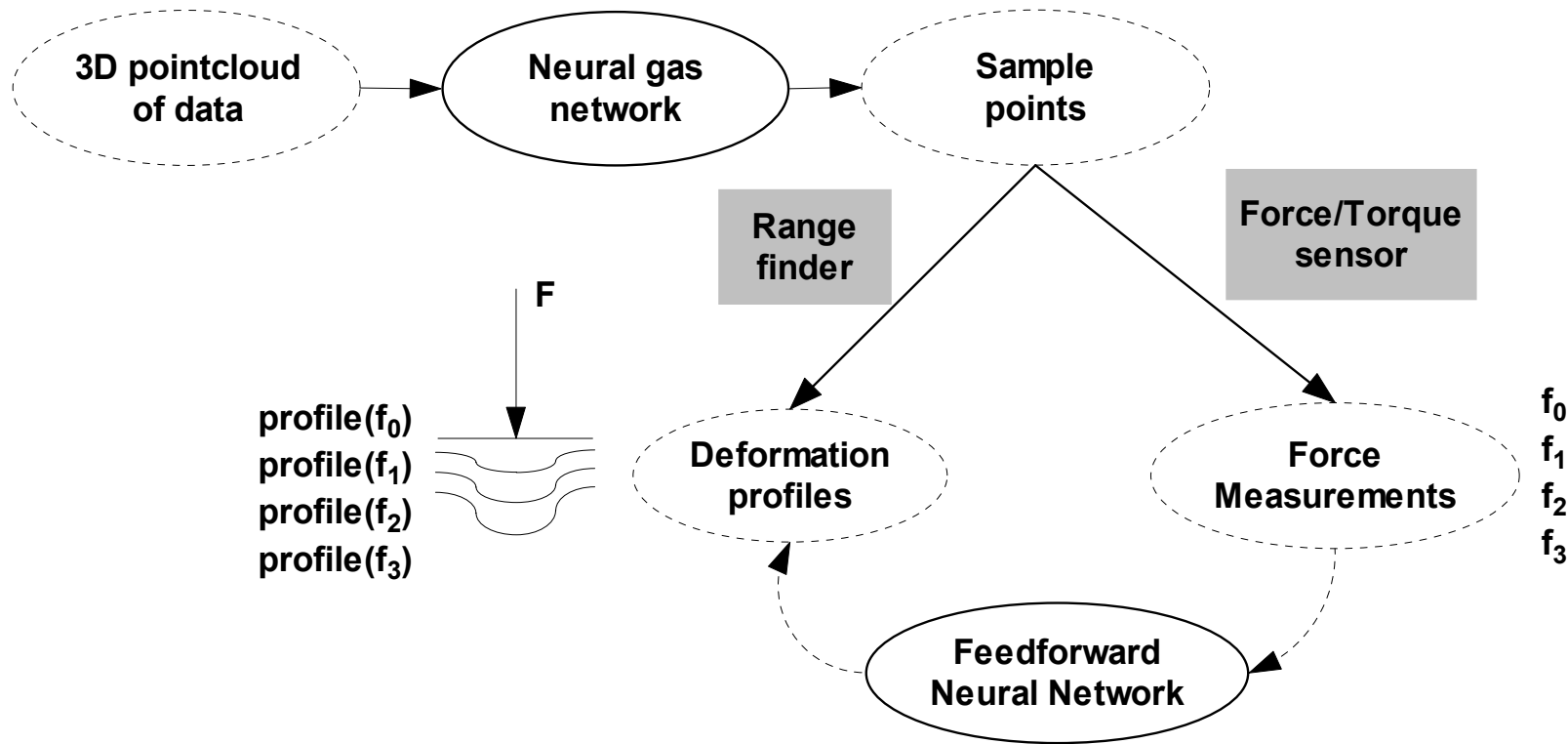
- For both, Neural Gas and SOM, networks the quality is improving with the number of training epochs



**On the whole the quality of the Neural Gas models appears to be better. Because of the boundary problem, the SOM models are to be avoided for non-noisy data.**

- Neural Gas and SOM neural networks are both able to compress the initial model with the desired degree of accuracy.
- The number of points can be further reduced by reducing the map size. However, there is a compromise to be made between the quality of the resulting compressed model and the map size.
- Neural Gas networks are able to model an entire scene of objects while the SOM networks are not able of such a performance.

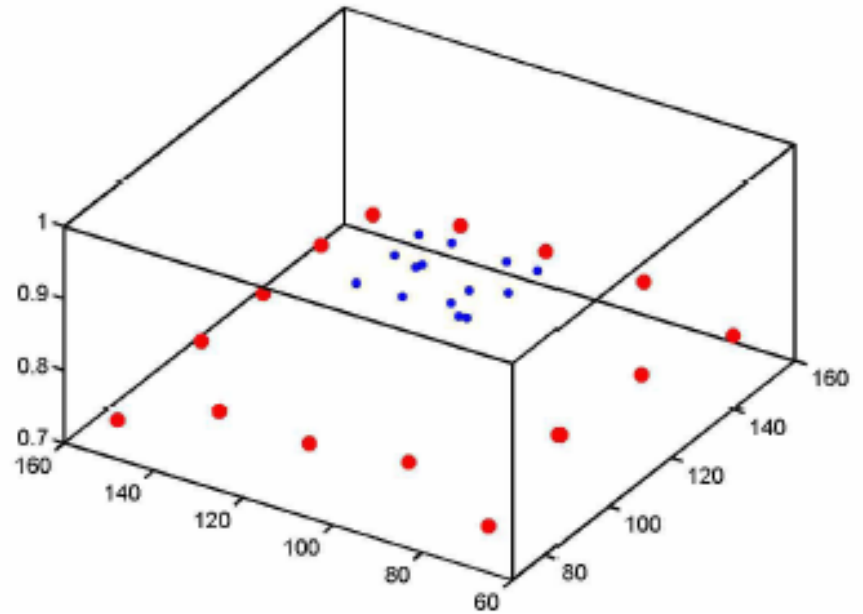
# Neural Network Mapping an Clustering of Elastic Behavior from Tactile and Range Imaging for Virtualized Reality Applications



Starting from a 3D point-cloud, a **neural gas NN** yields a reduced set of points on the 3D object's surface which are relevant for the tactile probing. The density of these tactile probing points is higher in the regions with more pronounced variations in the geometric shape. A **feedforward NN** is then employed to model the force/displacement behavior of selected sampled points that are probed simultaneously by a force/torque sensor and the active range finder.



Variable elasticity object used for experimentation.

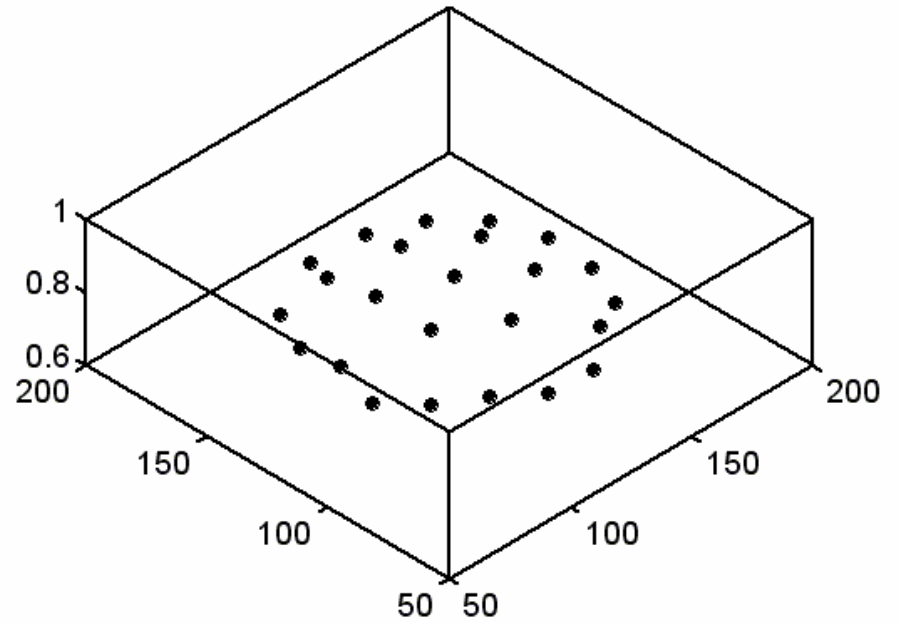


Sampling points selected with the neural gas network.

(from A.M. Cretu, E.M. Petriu, P.Payer "Neural Network Mapping and Clustering of Elastic Behavior from Tactile and Range Imaging for Virtualized Reality Applications," submitted to *IEEE Tr. Instr. Meas.*, Nov. 2006 ).

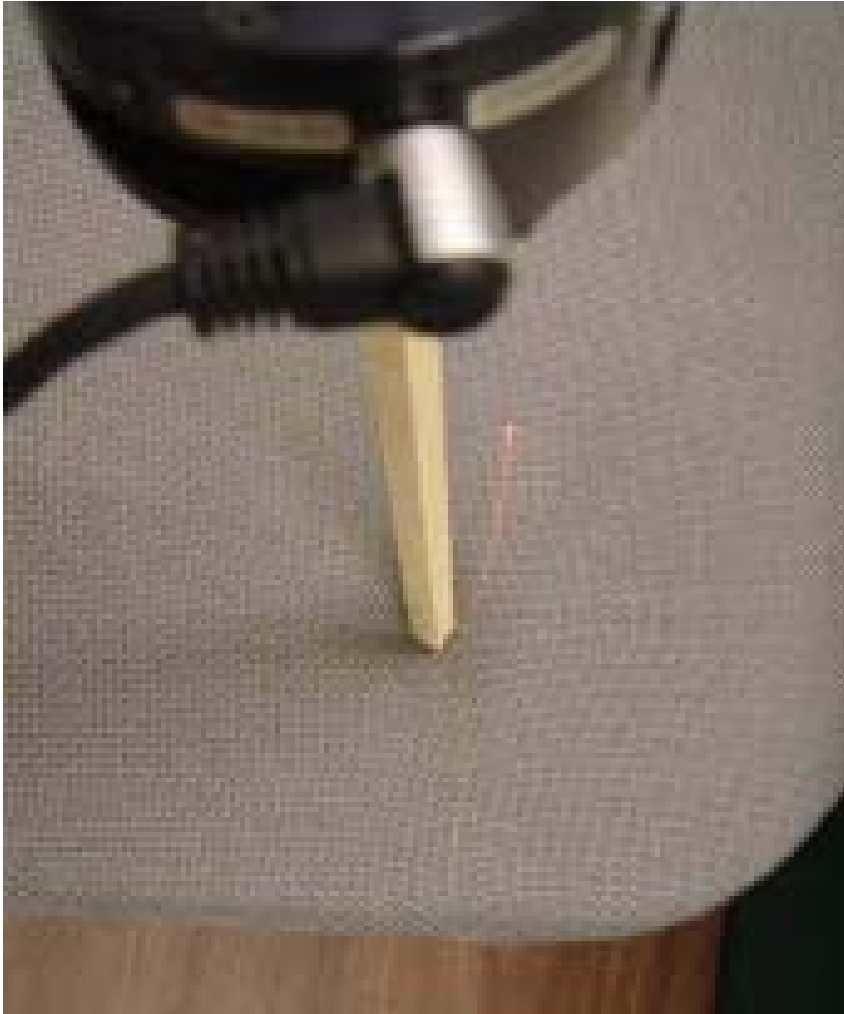


Elastic ball used for experimentation.



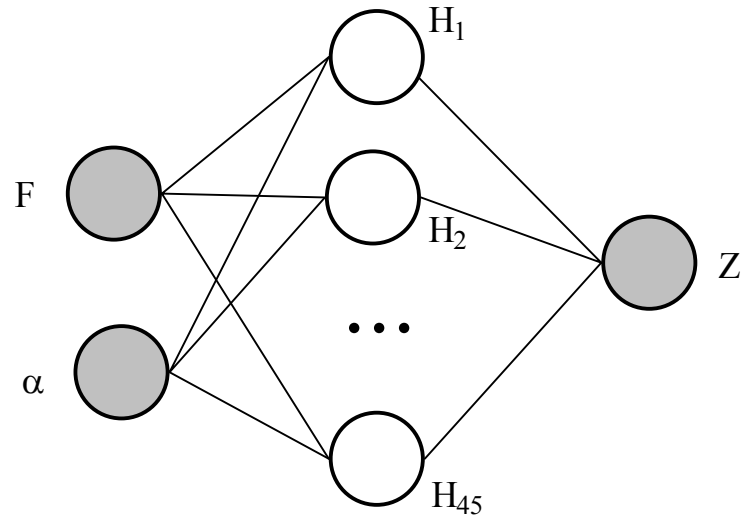
Sampling points selected with the neural gas network for the ball.

(from A.M. Cretu, E.M. Petriu, P.Payeur "Neural Network Mapping and Clustering of Elastic Behavior from Tactile and Range Imaging for Virtualized Reality Applications," submitted to *IEEE Tr. Instr. Meas.*, Nov. 2006 ).



Different magnitudes of a normal force are applied successively on the selected sampling points using the probe attached on the **force/torque sensor** and a range profile is collected with the **laser range finder** for each force magnitude.

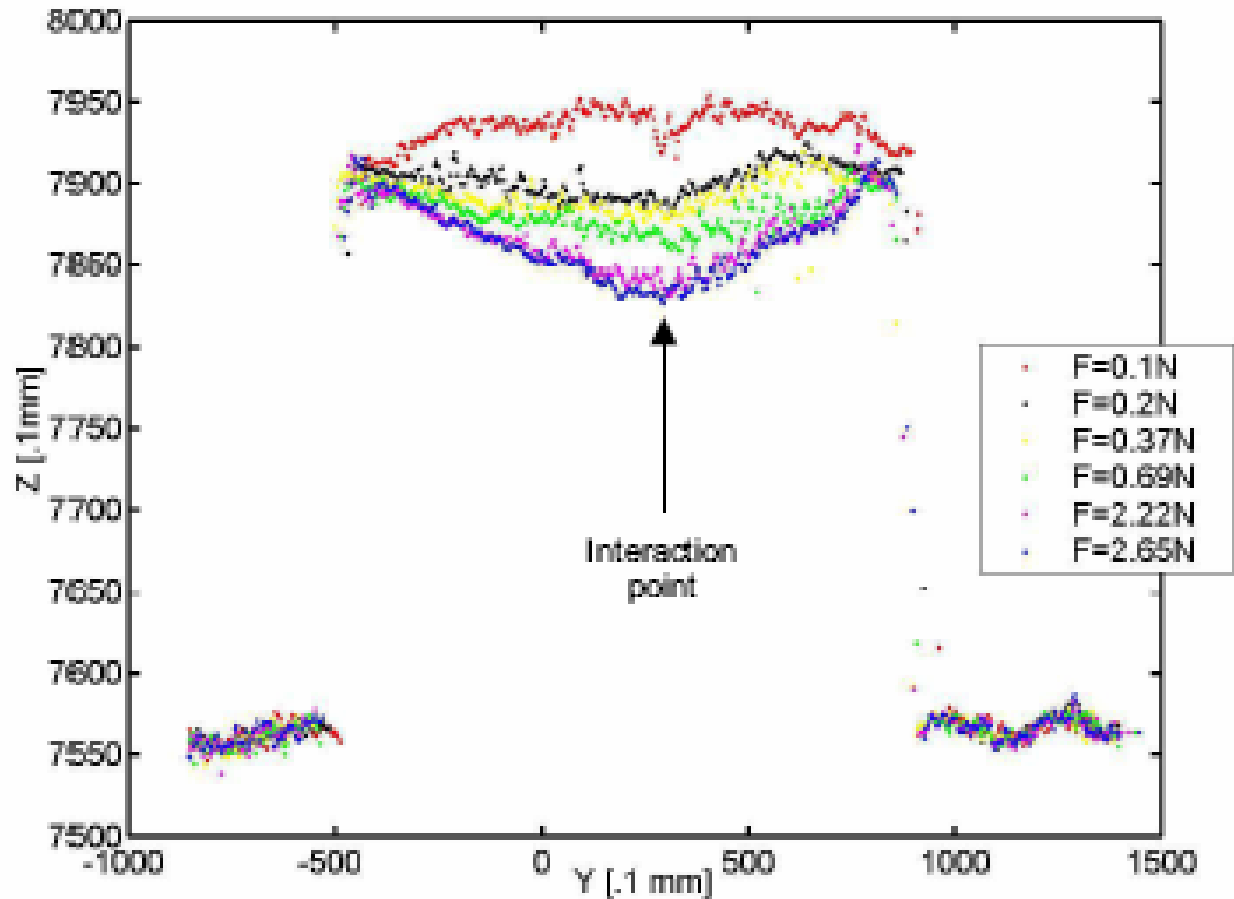
(from A.M. Cretu, E.M. Petriu, P.Payeur "Neural Network Mapping and Clustering of Elastic Behavior from Tactile and Range Imaging for Virtualized Reality Applications," submitted to *IEEE Tr. Instr. Meas.*, Nov. 2006 ).



There is no need to recover the explicit displacement information from the range profiles. Instead the NN models use the raw range data as a function of applied force,  $F$ , without explicitly defining values for the displacement. For each cluster of similar elasticity, a feed-forward NN with two input neurons ( $F$  and  $\alpha$ ), 45 hidden neurons ( $H_1$ - $H_{45}$ ) and one output neuron ( $Z$ ), is used to learn the relation between forces and the corresponding geometric profiles provided by the range finder.

The NN associated with each material were trained for 10,000 epochs using the Levenberg-Marquardt variation backpropagation algorithm with the learning rate set to 0.1. The whole data set is used for training in order to provide enough samples. The training takes approximately 10 min. on a Pentium IV 1.3GHz machine with 512MB memory. For the rubber, the sum-squared error reached during training is  $3.7 \times 10^{-3}$ , for cardboard is  $3.5 \times 10^{-2}$  while for the foam is  $2.2 \times 10^{-2}$ . As expected, the error is lower for the rubber where data is more compact and less noisy, while it remains slightly higher for the cardboard and even higher for the foam. But in all cases, excellent convergence is achieved.

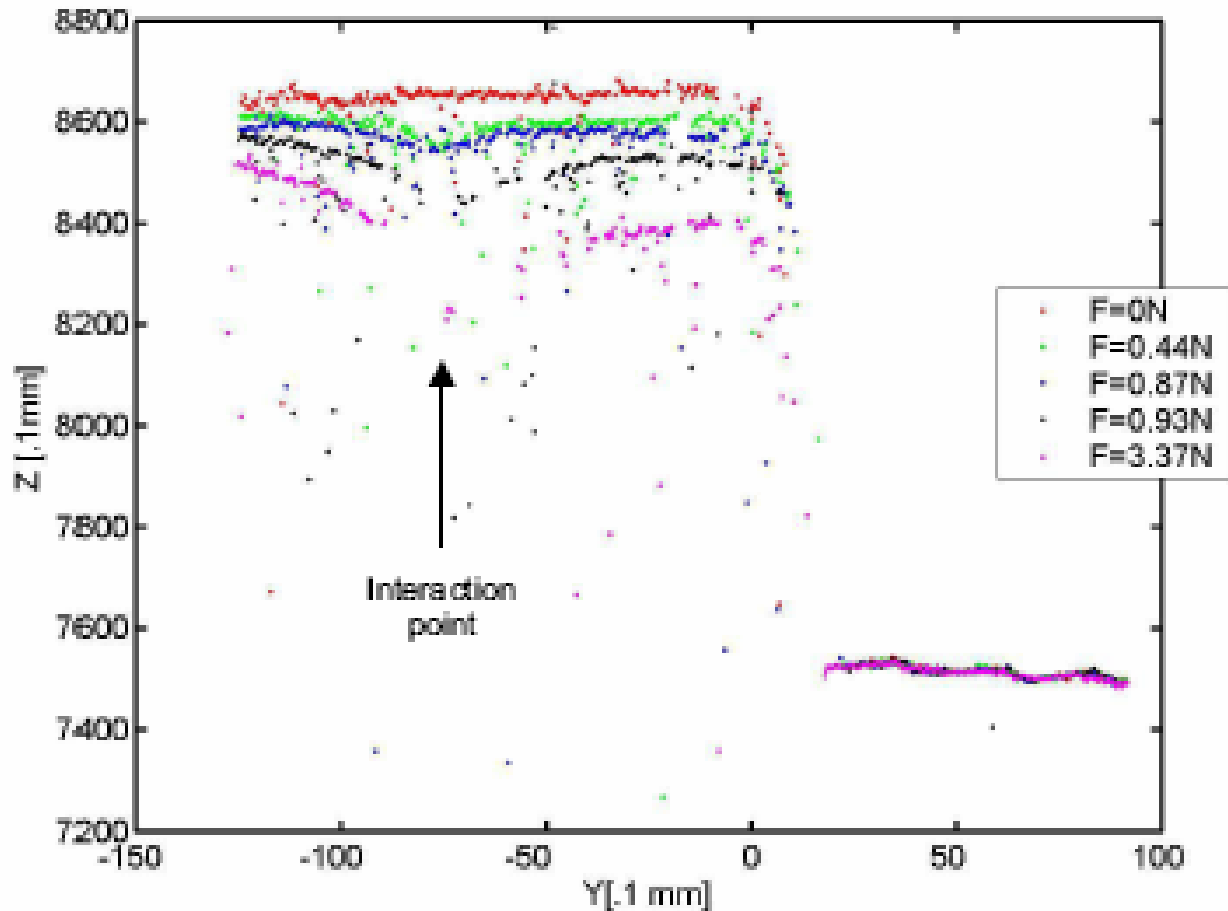
(from A.M. Cretu, E.M. Petriu, P.Payeur "Neural Network Mapping and Clustering of Elastic Behavior from Tactile and Range Imaging for Virtualized Reality Applications," submitted to *IEEE Tr. Instr. Meas.*, Nov. 2006).



Deformation profiles for semi-stiff material (cardboard).

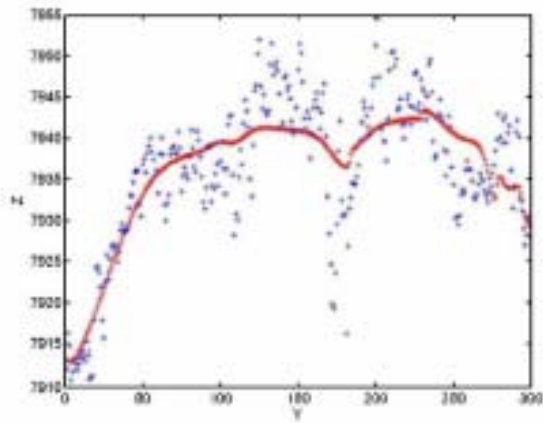
(from A.M. Cretu, E.M. Petriu, P.Payeur "Neural Network Mapping and Clustering of Elastic Behavior from Tactile and Range Imaging for Virtualized Reality Applications," submitted to *IEEE Tr. Instr. Meas.*, Nov. 2006).



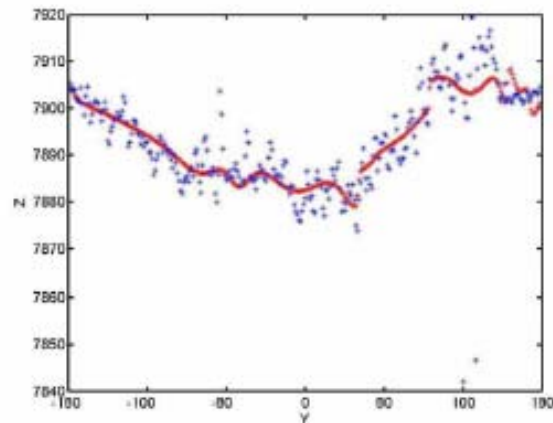


Deformation profiles for smooth material (foam).

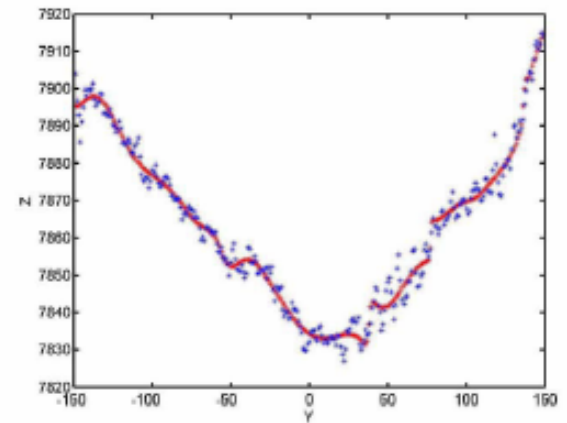
(from A.M. Cretu, E.M. Petriu, P.Payeur "Neural Network Mapping and Clustering of Elastic Behavior from Tactile and Range Imaging for Virtualized Reality Applications," submitted to *IEEE Tr. Instr. Meas.*, Nov. 2006).



(a)

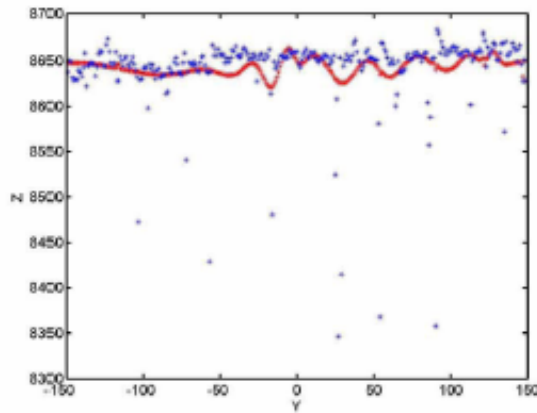


(b)

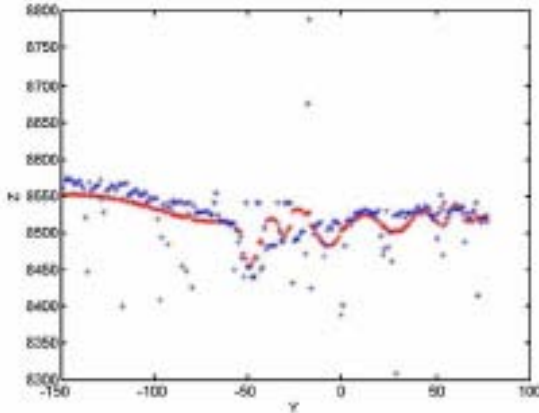


(c)

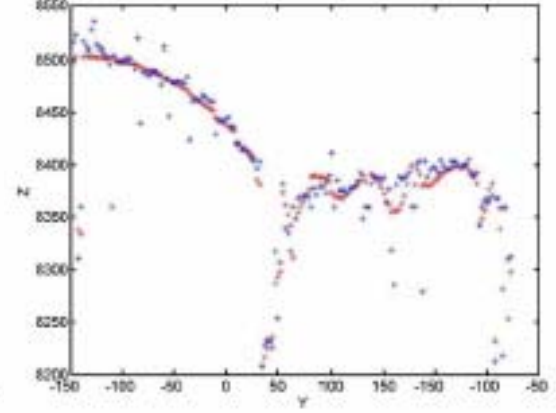
Real and modeled deformation curves using neural network for semi-stiff material (cardboard) under a normal force of: a)  $F=0.1\text{N}$ , b)  $F=0.37\text{N}$ , and c)  $F=2.65\text{N}$ .



(a)

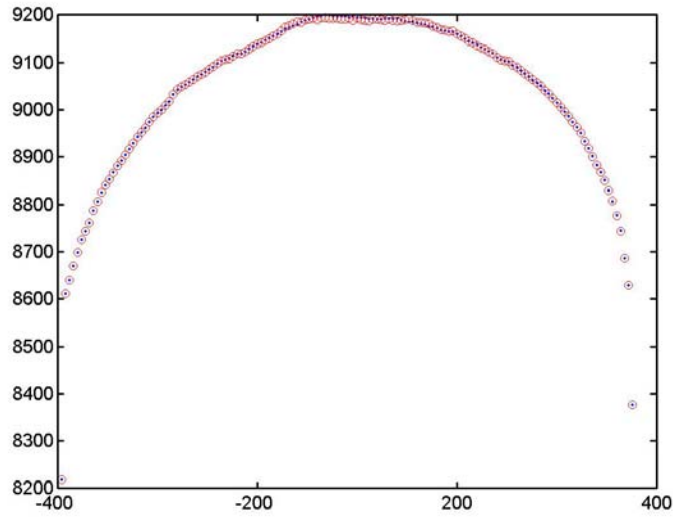


(b)

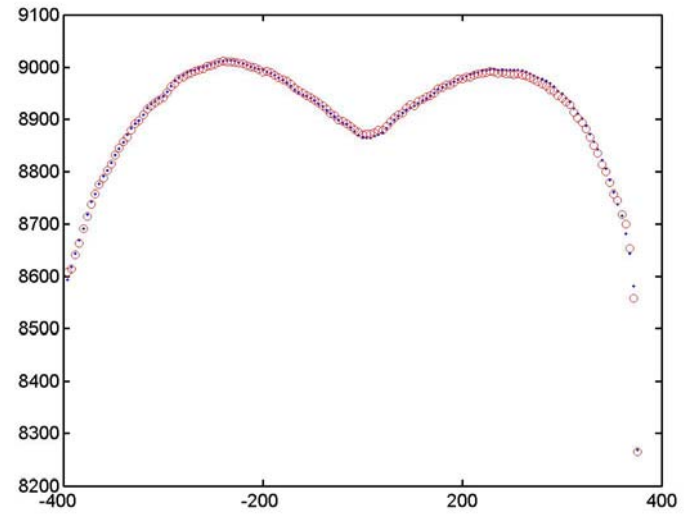


(c)

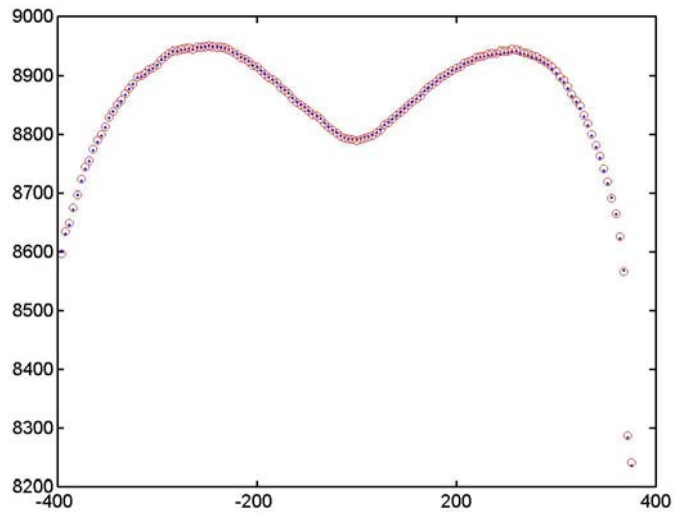
Real and modeled deformation curves using neural network for smooth material (foam) under a normal force of: a)  $F=0\text{N}$ , b)  $F=0.93\text{N}$ , and c)  $F=3.37\text{N}$ .



(a)

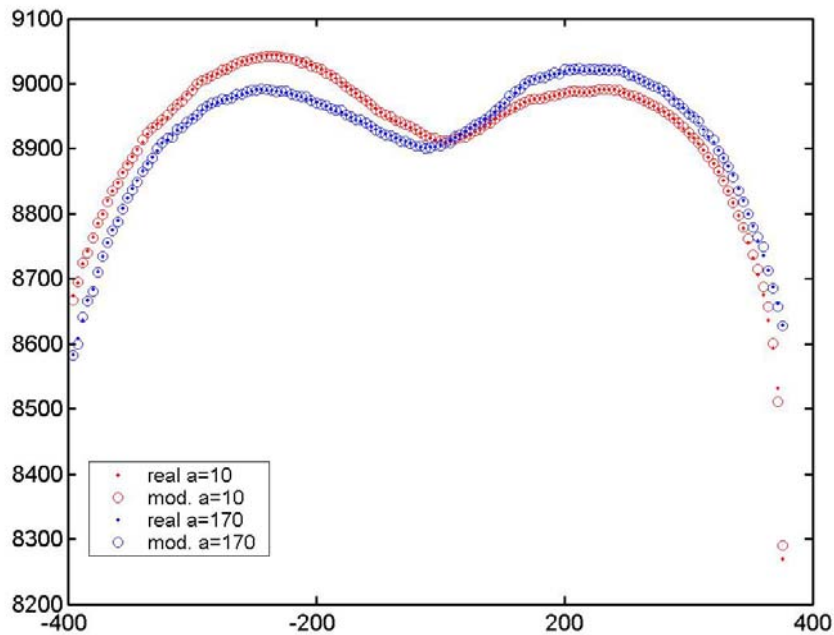


(b)

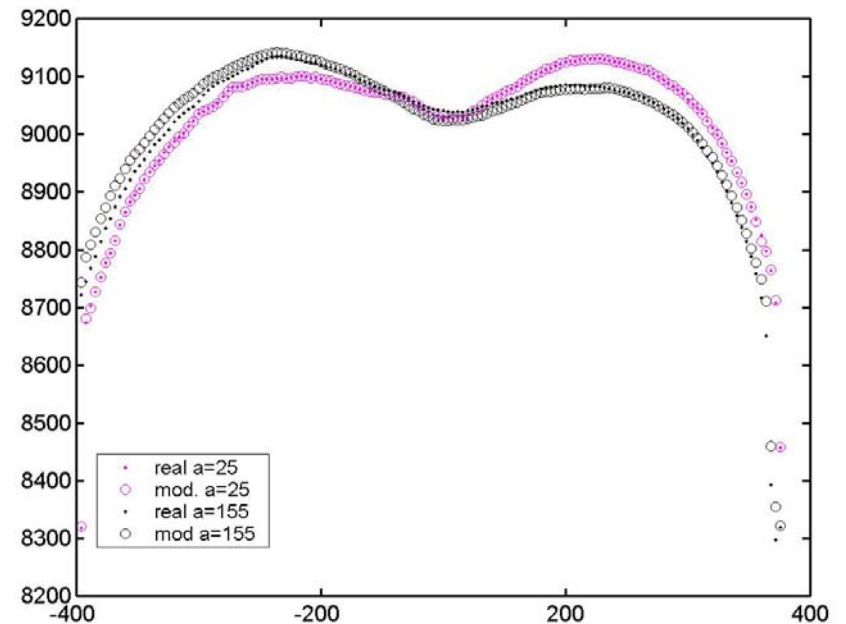


(c)

Real and modeled deformation curves using neural network for rubber under a normal force of:  
 a)  $F=0\text{N}$ , b)  $F=65.52\text{N}$ , and  
 c)  $F=80.5\text{N}$ .



(a)

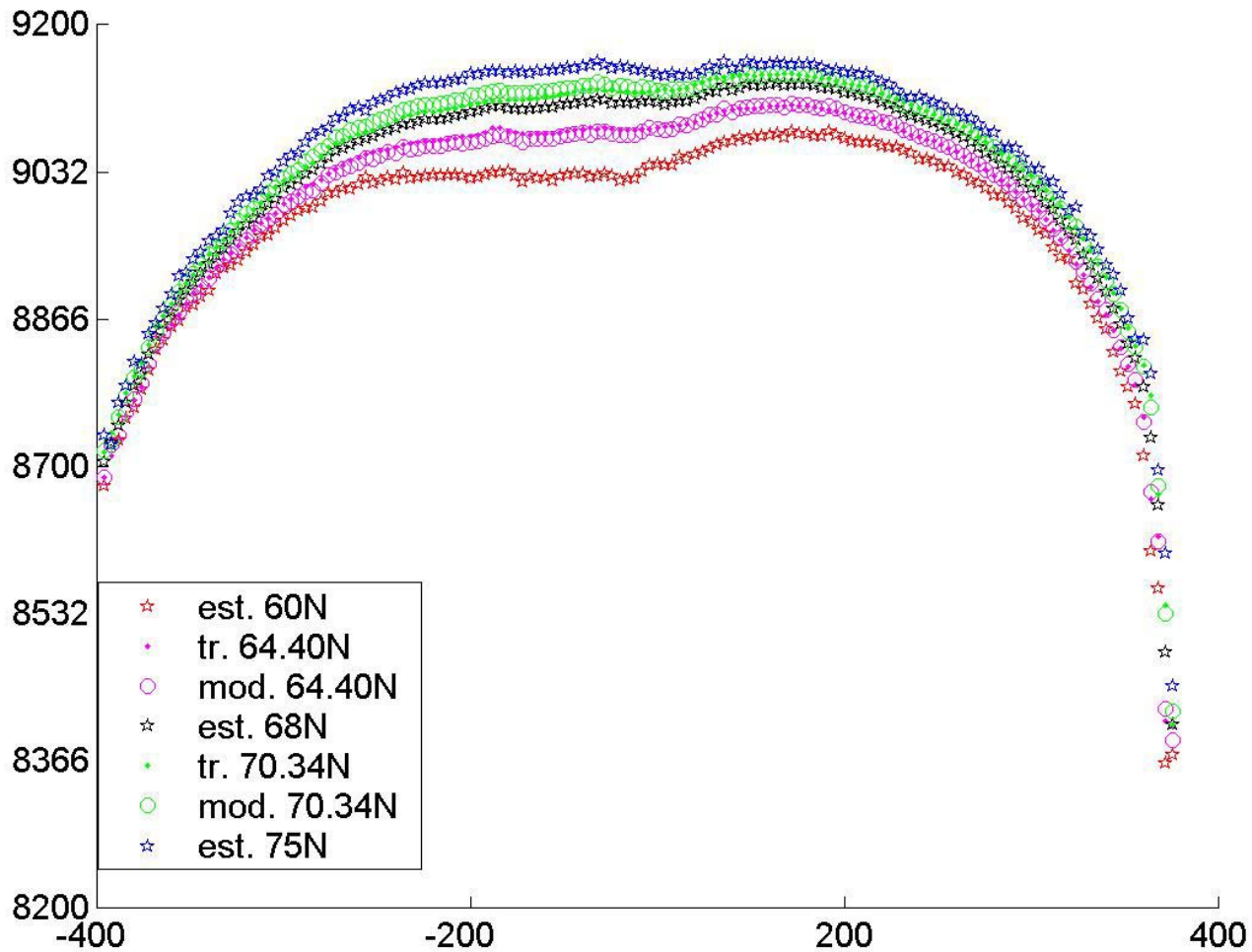


(b)

Real and modeled deformation curves using neural network for rubber under forces applied at different angles:

- a)  $F=65\text{N}$ ,  $\alpha_1=10^\circ$  and  $F=65\text{N}$ ,  $\alpha_2=170^\circ$ ,
- b)  $F=36\text{N}$ ,  $\alpha_1=25^\circ$ , and  $F=36\text{N}$ ,  $\alpha_2=155^\circ$

(from .A.M. Cretu, E.M. Petriu, P.Payer "Neural Network Mapping and Clustering of Elastic Behavior from Tactile and Range Imaging for Virtualized Reality Applications," submitted to *IEEE Tr. Instr. Meas.*, Nov. 2006).



Real, modeled and estimated deformation profiles detail of estimated deformation profiles using neural network for rubber ball for increasing forces applied at 75-degree angle.

(from A.M. Cretu, E.M. Petriu, P. Payeur "Neural Network Mapping and Clustering of Elastic Behavior from Tactile and Range Imaging for Virtualized Reality Applications," submitted to *IEEE Tr. Instr. Meas.*, Nov. 2006).

## Conclusions

- ❑ Tele-robotic dexterous manipulation requires not only specialized robotic hands with articulated fingers but also force, tactile, and kinesthetic sensors for the precise control of the forces and motions exerted on the manipulated object.
- ❑ More advanced haptic HCs, complementing the video HCs, need to be developed to allow human operators to have a telepresence experience virtually identical with what they would have had while manipulating real physical objects.
- ❑ NNs consisting of a collection of simple neuron circuits provide the massive computational parallelism offering efficient storage, model transformation, and real-time rendering capabilities for large numbers of composite geometric & haptic object models involved in the model-based interactive telemanipulation.
- ❑ Due to their continuous, analog-like, memory behavior, NNs are able to provide instantaneously an estimation of the output value for input values that were not part of the initial training set.

## Ottawa “U” Research Group – Relevant Graduate Theses

- C. Pasca, "*Smart Tactile Sensor*," M.A.Sc. Thesis, 2004.
- A.-M. Cretu, "*Neural Network Modeling of 3D Objects for Virtualized Reality Applications*," M.A.Sc. Thesis, 2003.
- A. Moica, "*Coprocessor for Decoding Multi-Valued Pseudo-Random Sequence Patterns*," M.A.Sc. Thesis, 2000.
- L. Zhao, "*Random Pulse Artificial Neural Network Architecture*," M.A.Sc. Thesis, 1998.
- S.S.K. Yeung, "*Model-Based Tactile Object Recognition Using Pseudo-Random Encoding*," Ph.D. Thesis, 1996.
- C. Archibald, "*A Computational Model for Skills-Oriented Robot Programming*," Ph.D. Thesis, 1995.
- D.M. Colven, "*Tactile Pattern Recognition Using Neural Networks*," M.A.Sc. Thesis, 1993.
- M. Greenspan, "*Robotic Active Tactile Skills*," M.A.Sc. Thesis, 1992.
- B. Karoui, "*Active Force Controlled Part Assembling for a Robotic Assembly Cell*," M.A.Sc. Thesis, 1988.

## Ottawa “U” Research Group - Publications in Haptics

- A.-M. Cretu, E.M. Petriu, “Neural-Network –Based Adaptive Sampling of Three Dimensional-Object Surface Elastic Properties,” *IEEE Trans. Instrum. Meas.*,” Vol. 55, No. 2, pp. 483 - 492, 2006.
- A.-M. Cretu, E.M. Petriu, G.G. Patry, “Neural-Network-Based Models of 3-D Objects for Virtualized Reality: A Comparative Study,” *IEEE Trans. Instrum. Meas.*,” Vol. 55, No. 1, pp.99-111, 2006.
- A.-M. Cretu, E.M. Petriu, P. Payeur, “Neural Network Mapping and Clustering of Elastic Behavior from Tactile and Range Imaging for Virtualized Reality Applications,” *Proc. IST 2006, IEEE Intl. Workshop on Imagining Systems and Techniques*, Minori, Italy, pp.17–22, April 2006.
- A.-M. Cretu, J. Lang, E.M. Petriu, “A Composite Neural Gas-Elman Network that Captures Real-World Elastic Behavior of 3D Objects,” *Proc. IMTC/2006, IEEE Instrum. Meas. Technol. Conf.*, pp. 1063-1068, Sorrento, Italy, April 2006.
- P. Payeur, C. Pasca, A.-M.Cretu, E.M. Petriu, “Intelligent Haptic Sensor System for Robotic Manipulation,” *IEEE Trans. Instrum. Meas.*, Vol. 54, No. 4, pp. 1583 – 1592, 2005.
- E.M. Petriu, S.K.S. Yeung, S.R. Das, A.-M. Cretu, H.J.W. Spoelder, “Robotic Tactile Recognition of Pseudorandom Encoded Objects,” *IEEE Trans. Instrum. Meas.*, Vol. 53, No. 5, pp. 1425-1432, 2004.



- E.M. Petriu, T.E. Whalen, V.Z. Groza, "Haptic Perception System for Robotic Tele-Manipulation," *Proc. INES 2002, 6th International Conference on Intelligent Engineering Systems 2002*, pp. 51-55, Opatija, Croatia, May 2002.
- S.K. Yeung, E.M. Petriu, W.S. McMath, D.C. Petriu, "High Sampling Resolution Tactile Sensor for Object Recognition," *IEEE Trans. Instrum. Meas.*, Vol. 43, No. 2, pp.277-282, 1994.
- W.S. McMath, M.D. Colven, E.M. Petriu, S.K. Yeung, "Tactile Pattern Recognition Using Neural Networks," *Proc. IEEE&SICE IECON'93 Conf.*, pp. 1391-1394, Maui, Hawaii, 1993.
- E.M. Petriu, W.S. McMath, "Tactile Operator Interface for Semi-autonomous Robotic Applications," *Proc. Int. Symposium on Artificial Intell. Robotics Automat. in Space, i-SAIRS'92*, pp.77-82, Toulouse, France, 1992.
- E.M. Petriu, W.S. McMath, S.K. Yeung, N. Trif, "Active Tactile Perception of Object Surface Geometric Profiles," *IEEE Trans. Instrum. Meas.*, Vol. 41, No. 1, pp.87-92, 1992.
- S.K. Yeung, W.S. McMath, E.M. Petriu, N. Trif "Three Dimensional Object Recognition Using Integrated Robotic Vision and Tactile Sensing,"*Proc. IEEE&RSJ Int. Workshop on Intell. Robots and Systems IROS'91*, pp.1370-1373, Osaka, Japan, 1991.
- E.M. Petriu, D.C. Petriu, V. Cretu, "Control System for an Interactive Programmable Robot," *Proc. CNETAC Nat. Conf. Electronics, Telecommunications, Control, and Computers*, pp.227-235, Bucharest, Romania, Nov. 1982.

## References

- J. Lederman, et al., "Lessons From the Study of Biological Touch for Robotic Haptic Sensing", in *Advanced Tactile Sensing for Robotics* (H.R. Nicholls, ed.), World Scientific, 1992.
- M.H. Lee, H.R. Nicholls, "Tactile Sensing for Mechatronics - a State of the Art Survey," *Mechatronics*, 9(1999), pp. 1-31, 1999.
- M.J. McDonald, *Active Research Topics in Human Machine Interfaces*, Sandia Report, SAND2000-2779, Dec. 2000.
- X. Di, et al., " Sensor-Based Hybrid Position/Force Control of a Robot Manipulator in an Uncalibrated Environment," *IEEE Trans. Contr. Syst. Technol.*, Vol. 8, No. 4, 635 – 645, 2000.
- A.M. Okamura, N. Smaby, M.R. Cutosky, "An Overview of Dexterous Manipulation," *Proc.ICRA'00 - IEEE Intl. Conf. Robot. Autom.*, pp. 255–262, Apr. 2000.
- G. Robles-De-La-Torre, V.Hayward "Force Can Overcome Object Geometry In the perception of Shape Through Active Touch", *Nature*, 412 (6845), pp. 445-8, 2001
- A.M. Okamura, et al., "Reality-Based Models for Vibration Feedback in Virtual Environments," *IEEE/ASME Trans. Mechatronics*, Vol. 6, No. 3, pp. 245-252, 2001.

- R.W. Harrigan, P.C. Bennett, *Dexterous Manipulation: Making Remote Manipulators Easy to Use*, Sandia Report, SAND2001-3622, Nov. 2001.
- P.C. Bennett, R.J. Anderson, *Robotic Mobile Manipulation Experiments at the US Army Maneuver Support Center*, Sandia Report, SAND2002-1779, June. 2002
- G. Burdea and Ph. Coiffet, *Virtual Reality Technology* (2nd edition), Wiley, NJ, 2003.
- M. Benali-Khoudja, et al., "Tactile interfaces: A state-of-the Art Survey," *Proc. ISR 2004 -35th Intl.Symp. Robotics*, Paris, March 2004.
- K. Salisbury, F. Conti, F. Barbagli, "Haptic Rendering: Introductory Concepts," *IEEE Computer Graphics and Applications*, Vol. 24, No. 2, pp. 24 – 32, 2004.
- C. Sung-Ouk, A.M. Okamura, "Impedance-Reflecting Teleoperation with a Real-Time Evolving Neural Network Controller," *Proc. IROS 2004 - Intl. Conf. Intel. Rob. Syst.*, pp. 2241–2246, 2004.
- M. Mahvash, V. Hayward, "High-Fidelity Passive Force-Reflecting Virtual Environments," *IEEE Trans. Robotics*," Vol. 21, No. 1, pp.38-46, 2005.
- G. Cini et al., "A novel fingertip haptic device for display of local contact geometry," *Proc. WHC 2005 - First Joint Eurohaptics Conf. and Symp. Haptic Interfaces for Virtual Environment and Teleoperator Systems*, pp. 602 – 605, March 2005.
- G. Robles-De-La-Torre, "The Importance of the Sense of Touch in Virtual and Real Environments", *IEEE Multimedia*, 13(3), 2006, Special issue on Haptic User Interfaces for Multimedia Systems, pp. 24-30.

***Thank You !***